Autostereoscopic Projection Display using Rotating Screen

by

Osman Eldeş

A Thesis Submitted to the
Graduate School of Sciences and Engineering
in Partial Fulfillment of the Requirements for
the Degree of

Master of Science

in

Electrical and Electronics Engineering

Koç University

January, 2016

Koç University

Graduate School of Sciences and Engineering

This is to certify that I have examined this copy of a master's thesis by

Osman Eldeş

and have found that it is complete and satisfactory in all respects,
and that any and all revisions required by the final
examining committee have been made.

Committee Members:

_____

Prof. Hakan Urey

_____

Assoc. Prof. Göksenin Yaralıoğlu

_____

Asst. Prof. Fehmi Çivitci

Date: _____

Dedicated to Ali Kangel Beyağabey,

ABSTRACT

A new technique for glasses-free (auto-stereoscopic) and multi-view 3D display is proposed and demonstrated in this thesis. The technique uses two mobile projectors, a rotating retro-reflective diffuser screen rotated by a mechanical unit, a pupil-tracking camera and a computer. Two mobile projectors project stereo images onto a transfer screen composed of a retro-reflector and a 1D diffuser. The transfer screen forms two viewing slits through each of which only one image of stereo image pair is seen. The mechanical unit rotates the transfer screen around its center according to the viewer's position obtained by the pupil tracker. As the screen is rotated accordingly, the viewing slits track the viewer's eyes. Thus, a single viewer can perceive 3D in a large viewing field. Images from different perspectives can be presented to the viewer using the information from the pupil-tracker. Advantages of the proposed technique compared to conventional autostereoscopic projection displays are as follows: it requires only two projectors rather than an array of projectors; there is no image registration problem on the screen once the projectors are aligned; the viewing slits remain aligned with the viewer's pupils, thus the viewer never perceives discrete transitions between different perspectives; the technique can provide high-gain, and sufficient brightness using low-power mobile projectors. In order to demonstrate capabilities of the proposed technique, a prototype was developed. The prototype consists of two laser based pico projectors using MEMS scanners , a retro-reflective diffuser screen as a transfer screen, pupil-tracker, rotating mechanism which rotates the transfer screen around its center, and a personal computer to provide content and closed-loop control of the tracker and the screen. The resulted prototype presents stereo images to a single viewer without need of any glasses. The screen is circular with 60cm diameter and the image is a rectangular image that fits on the screen and viewed from about 100cm

distance. The prototype allows the viewer to move approximately 70 cm along the horizontal axis, and 50 cm along the vertical axis with an average crosstalk below %5. The display quality in terms of brightness and crosstalk has been measured and reported for different types of light diffusers.

ÖZETÇE

Bu tez içerisinde çoklu görüntülü gözlüksüz 3 boyutlu ekranlar için yeni bir teknik geliştirildi. Geliştirilen teknik iki adet taşınabilir projektör, bir adet merkezi etrafında dönen retro-yansıtıcılı ışık dağıtıcı ekran, göz takip kamerası, ve bir adet bilgisayar kullanmaktadır. Taşınabilir projektörler retro-yansıtıcı ve ışık dağıtıcıdan oluşan ekran üzerine 3 boyutlu görüntüyü yansıtmaktadır ve ekran iki adet izleme şeridi oluşturmaktadır. Bir izleme şeridinden sağ göz için gerekli 3B görüntü görülmekte iken diğer izleme şeridinden ise sol göz için gerekli 3B görüntü görülebilmektedir. Mekanik aksam göz takip kamerasından alınan bilgiye göre ekranı merkezi etrafında döndürmektedir ve bu dönüş sayesinde izleme pencereleri de izleyicinin gözlerinin üzerine gelecek şekilde izleyiciyi takip etmektedir. Bu şekilde bir adet izleyici geniş bir alanda gözlük takması gerekmeden 3B görüntüyü izleyebilmektedir. Göz takip kamerası vasıtasıyla kullanıcının konumuna göre farklı açılardan 3 boyutlu görüntüler kullanıcıya sunulabilmektedir.

Geliştirilen tekniğin benzer tekniklere göre avantajları şunlardır; bir dizi projektör kullanmak yerine sadece iki adet projektör kullanması, yansıtılan görüntülerde mekanik hareketten kaynaklanan herhangi bir bozulma olmaması, izleme şeritleri daima izleyicinin gözlerinin üzerinde oluştuğu için izleyicinin hareketlerinden ötürü görüntü kaybı yaşanmaması, sadece iki adet düşük güçlü taşınabilir projektör kullanmasına rağmen yüksek kazanım ve parlaklık sağlaması.

Geliştirilen teknik kullanılarak bir adet prototip üretilmiştir. Üretilen prototip iki adet lazer tabanlı Mikro-Elektro Mekanik Tarayıcı kullanan piko projektör, retro yansıtıcı ve ışık dağıtıcıdan oluşan ekran, göz takip kamerası, ekranı merkezi etrafında döndüren mekanik aksam, projektörlere içerik sağlayan ve kullanıcı konumuna göre ekranı döndürme komutu veren bir adet bilgisayardan oluşmaktadır. Üretilen prototip

bir adet izleyiciye yatay eksende 70 cm, dikey eksende 50 cm hareket özgürlüğü sağlayarak ve herhangi bir gözlük takmasını gerektirmeden 3B görüntüyü sunmaktadır. Oluşturulan ekran 60 cm köşegen uzunluğuna sahip altıgen şeklinde olup üzerine yansıtılan görüntüler 100 cm uzaklıktan izlenmektedir. İzleme alanı içerisinde sağ göz resmi ve sol göz resmi arasındaki gürültü değeri %5'in altındadır. Parlaklık ve gürültü değeri cinsinden farklı ışık dağıtıcılar kullanılarak ekran kalite testleri yapılmıştır ve rapor edilmiştir.

ACKNOWLEDGEMENTS

I am very grateful to my supervisor, Prof. Hakan Ürey for giving me a chance to be a OML research member. Through all these years, i have learned so much from him in research and life perspective. His admirable approach to young researchers must be acknowledged.

I am thankful to my dear colleagues at OML: Kaan Akşit and Selim Ölçer. They were always helpful in many ways, and provided a good team spirit with an endless effort. I am also thankful to previous and current members of OML. I really enjoyed being in a group with Onur Çakmak, Erhan Ermek, Kıvanç Hedili, Ulaş Adıyan Başarbatu Can, Uğur Aygün and Sven Holmström.

I am also thankful to Assoc. Prof. Göksenin Yaralıoğlu and Asst. Prof. Fehmi Çivitci for taking part in my thesis committee.

I acknowledge that the whole research through my MSc studies would not have been possible without the financial support of TÜBİTAK.

Finally, i am very grateful to my family for endless support they have given me during my life, and believing in me in all those years. It would be impossible to complete this thesis without the support of my family.

TABLE OF CONTENTS

LIST OF TABLES

LIST OF FIGURES

NOMENCLATURE

$3D$	:	Three dimensional
$1D$	:	Single Dimensional Diffuser
IPD	:	Interpupillary distance
$MEMS$	:	Micro electromechanical system
$SS3D$	:	Super Stereoscopic 3D
OML	:	Optical Microsystems Laboratory
$FWHM$	:	Full width at half max
$FWZI$	:	Full width at zero intensity
LSD	:	Light Shaping Diffuser

Chapter 1

INTRODUCTION

Autostereoscopic displays present stereoscopic images to viewers without need of any special user-mounted device. Human brain interprets the three-dimensional (3D) structure of a stereoscopic image by some perceptual cues, such as stereo parallax, movement parallax, accomodation, and convergence. 3D displays (autostereoscopic and stereoscopic) provide at least stereo parallax to present stereoscopic images to the viewers, [4]. Stereo parallax means that each eye of the viewer sees different perspective of the 3D scene. Stereoscopic displays requires viewers to wear a special glasses for providing stereo parallax. This special glasses allows only one perspective to pass through for each eye. In contrast autostereoscopic displays do not require any special glasses to provide stereo parallax, but they control the light path so that each eye of the viewer sees different perspective of the stereoscopic image. By controlling the light path, autosteresocopic displays form exit pupils, so called viewing slits through each of which different perspectives are visible. These viewing slits are either fixed where the viewers' left/right eyes must be positioned or dynamically follow viewers' eye pupils under the control of a pupil-tracker.

There are several different transfer screens to control light path and form viewing slits. These transfer screens are parallax barrier based screens, lenticular screens, Fresnel lens (pupil forming screen) in front of a light shaping diffuser or retro-reflective light diffusing screens.

In all transfer screens mentioned so far, except parallax barrier, in order to present stereoscopic images to the viewer in a comfortable viewing area, either tens of viewing slits must be formed which requires multiple projectors to be used or viewing slits

must dynamically follow the viewers' pupils which requires projectors to be moved accordingly. These solutions have some drawbacks. If multiple projectors are used, using many projectors will cause high cost, complex system structure, and image registration problem. In the case of moving projectors, image registration problem, which is the problem of projecting images on the substantially overlapping areas of the screen, and correcting the image distortions, will occur in every movement of projectors.

Another problem with the multiple projector method and the parallax barrier method is that they create discrete viewing slits. Thus, when the viewer changes its position, viewer experiences discrete transitions between viewing slits, and it causes unnatural 3D experience.

Motivation of the thesis is to introduce an autostereoscopic display method, which aims to solve all aforementioned problems and presents a high quality 3D experience. To do so, we have introduced a novel autostereoscopic projection display method which employs a pair of projectors, a pupil-tracker and a rotating transfer screen to form a pair of dynamic viewing slits aligned with the viewers eyes. Any of the aforementioned transfer screens, except parallax barrier, can be used for the proposed technique. The viewing slits track the viewers eyes in a large viewing field by rotating the transfer screen in-plane. The present method has advantages over conventional autostereoscopic projection displays in terms of number of projectors, transition between different perspectives, and the image registration on the screen. The method employs two projectors rather than an array of projectors, which decreases the cost, and complexity of the display. In the present method, there is no loss of 3D vision and discrete transition between different perspectives when the viewer changes his position. In the present method, since neither projectors nor screen make translational movement, projected images are always overlapped on the screen, and no distortion correction is required. The method can provide high-gain, and sufficient brightness even with a pair of mobile projectors. The main limitation of this technique is that it is suitable for only one viewer.

A working prototype of the proposed technique which uses retro-reflective light diffusing screen as transfer screen has been constructed. Luminance, crosstalk, and dynamic viewing area analysis have been performed. The prototype provides a viewing field which has 700 mm horizontal length, and 500 mm vertical length. The average crosstalk value along the viewing field is below % 5 which is the maximum value in order to prevent reduced viewing comfort in half of population according to [5].

For a possible new application and solving a well-known problem of accomodation-vergence conflict of conventional stereoscopic displays, a new technique named as Super Stereoscopy (SS3D) which has been developed in our group, Optical Microsystems Laboratory (OML), are tested with the proposed display, as reported in [3]. By adding a specially developed glasses to the proposed display, the viewer perceives stereo image without any accomodation-vergence conflict. The detailed analysis is explained in [2].

In chapter 2, the related works found in the literature will be reviewed. Transfer screen examples will be presented. In chapter 3, the concept of the proposed method, characterization of the display, works that have been carried to build a working prototype, and display quality measurements, such as luminance, crosstalk measurements will be presented.

1.1 Contribution of The Thesis Research

The most important contribution of the thesis is that a novel autostereosopic projection display technique was conceived, developed, and demonstrated for the first time during this thesis research. Our approach has advantages over conventional autostereoscopic display approaches as detailed in Chapter 2. A patent, title Method for Autostereoscopic Displays was filed, [6] during the thesis study as the sole inventor and it has been licensed to Inventram for commercialization. The technique was first reported as a journal paper in Optics Express, [7] and the article was promoted by the Optical Society of America's Spotlight on Optics, [8]. The proposed technique was presented in 3 different conferences, [9–11]. Overall, a journal paper, 3 conference papers and a patent has been published as the outcome of the thesis.

The prototype developed in this thesis study provides very good image quality and competes well with other commercial 3D systems. When our group needed an auto-stereoscopic display system to demonstrate a new technique called super stereoscopic multi view, the team used the prototype developed in this research and achieved very good results, [2].

Chapter 2

AUTOSTEREOSCOPIC PROJECTION DISPLAYS

Autostereoscopic displays create virtual viewing slits, through which intended perspective images can be presented. Through these viewing slits, right and left eye of the viewer see different perspective images, and viewer perceives stereo image without the need of glasses. There are several different methods to create virtual viewing slits. These methods utilize parallax barrier, lenticular lenslet, Fresnel lens (pupil forming screen), retro-reflective light diffusing material, or light shaping diffuser (LSD) technology. The created viewing slits can be either fixed, or can dynamically follow viewers pupil position under the control of a pupil-tracker. In this chapter, related autostereoscopic display methods in the literature will be examined.

2.1 Parallax Barrier Displays

In parallax barrier based displays, right and left eye images are interlaced in columns on the display, typically an LCD display. A parallax barrier is positioned in front of the display so that it creates vertical viewing slits for right eye and left eye, separately. Created right and left eye viewing slits are repeated horizontally along the viewers space. Thus, as long as the viewers right eye is in the right eye viewing slit, and left eye is in the left eye viewing slit, the viewer perceives 3D. In [1], parallax barrier is used to build an autostereoscopic display. It must be noted that this is not the only way of parallax barrier usage.

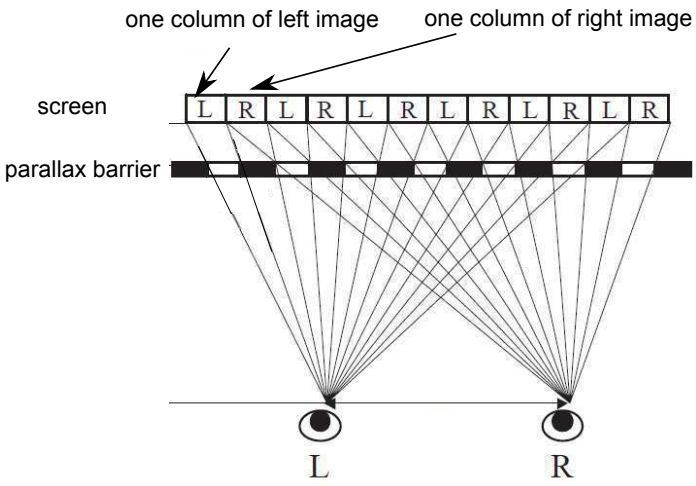

Figure 2.1: A parallax barrier screen [1].

2.2 Lenticular Screen

Lenticular screens can be used as in parallax barrier case. The horizontally interlaced right and left images on the display are diffused by the lenticular screen so that right eye image pixels can be seen only in the right eye viewing slits and left eye image pixels can be seen only in the left eye viewing slits. Thus, viewer can perceive 3D as long as viewers right and left eye are in the corresponding viewing slits. In [12], the mentioned method is utilized.

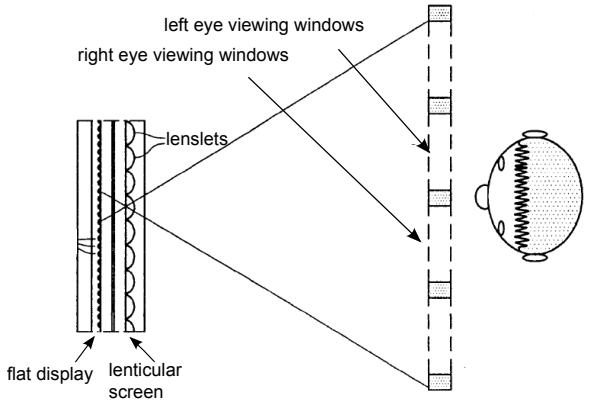

Figure 2.2: Lenticular screen with a flat display.

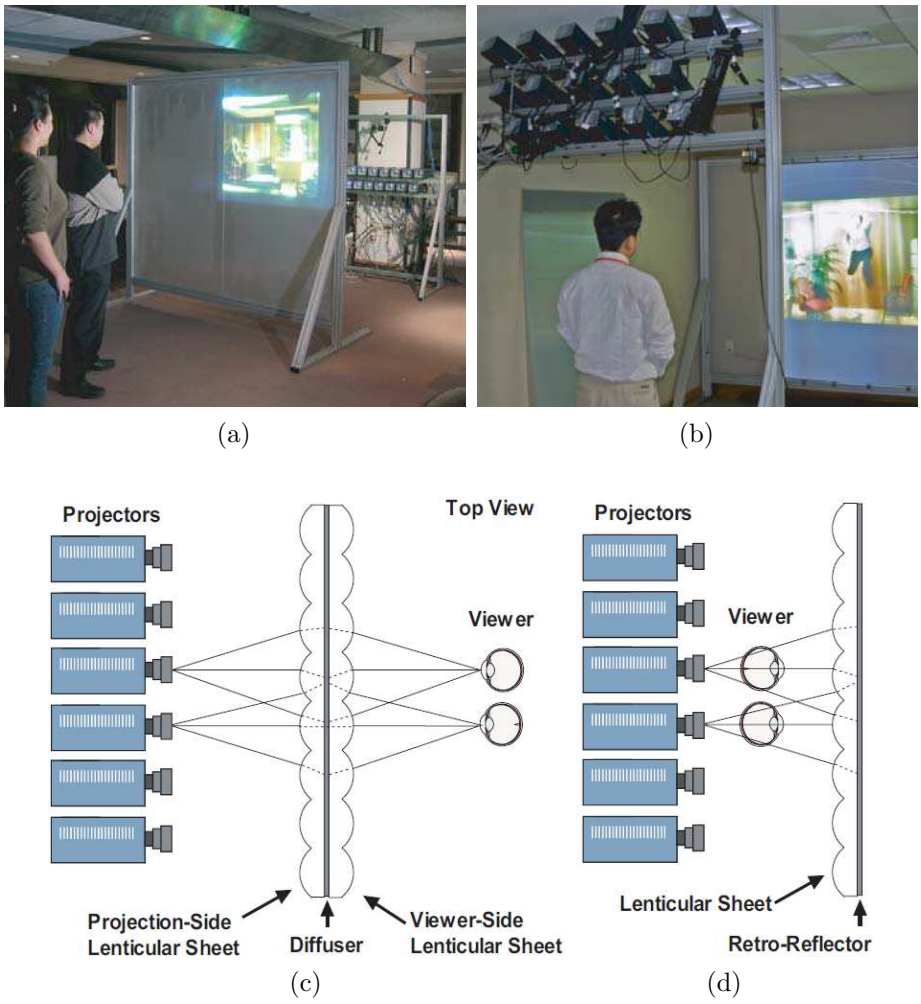

Figure 2.3: Different usage of lenticular screen in a projection based autosteresocopic displays. (a) Rear-projection 3D display with double-lenticular screen (b) Front-projection 3D display with single-lenticular screen (c) Rear-projection system sketch (d) Front projection system sketch.

One of lenticular screen usages in autostereoscopic displays is based on the optical property that lenticular screens can be used to retro-reflect projected light back to the source, horizontally. [13] describes a lenticular lenslet based display method which utilizes the mentioned optical property. Since each single lenticule in lenticular screen focuses light in only one direction, which is horizontal direction in the mentioned patent, lenticular screen creates vertical viewing slits, in which the image projected by the corresponding projector is presented. By placing multiple projectors, which are

horizontally apart from each other, not more than an average human interpupillary distance (approximately 65 mm), multiple vertical viewing slits are created in the viewers space. Through each vertical viewing slit, the perspective image projected by the corresponding projector can be seen. Thus, the viewer perceives stereo images in the viewers space . It must be noted that instead of placing multiple projectors horizontally apart from each other, two projector could be used and horizontally move according to the position of viewer.

Another usage of lenticular screens is placing a diffuser between two lenticular screens, as in [14]. The constructed screen is called as double lenticular screen and it is used in the rear projection displays. A projector projects image onto the double lenticular screen. The lenticular screen, in the projector side, focuses light as thin vertical stripes onto the diffuser. The lenticular screen, in the viewer side, diffuses vertical stripes on the diffuser, such that the projected image can be seen only in a narrow vertical viewing slit. Thus, by placing multiple projectors horizontally apart from each other and creating multiple viewing slits, or by moving two projectors according to the position of viewer, viewer can perceive 3D.

2.3 Fresnel Lens Based Autostereoscopic Displays

In fresnel lens based displays, a vertically aligned single dimensional (1D) diffuser is placed onto Fresnel lens, [15]. The Fresnel lens focuses the projected image by projector, and then diffuser diffuses this focused image into a vertical viewing slit. By placing multiple projectors horizontally apart from each other or by moving two projectors according to the position of viewer, viewer can perceive 3D through these created viewing slits. It must be noted that this is not the only method to make use of Fresnel lens in autostereoscopic displays.

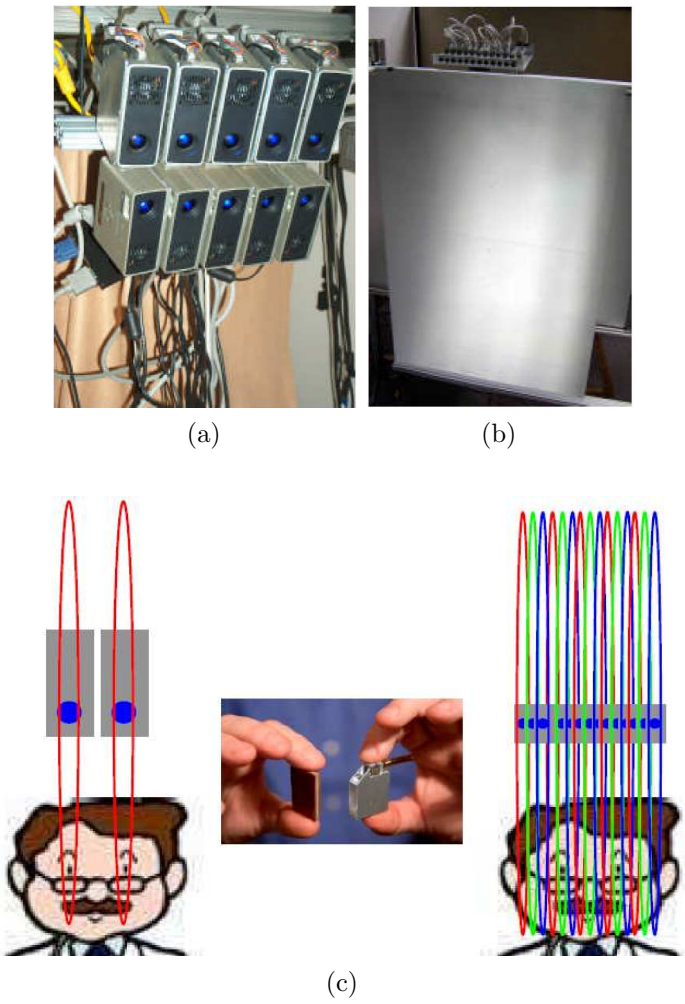

Figure 2.4: Retro-reflective light diffusing screen used with projector array. (a) Projector array (b) Retro-reflective light diffusing screen (c) The system sketch showing created viewing slits.

2.4 Retro-reflective Diffusing Material

A retro-reflective light diffusing material can be used to create viewing slits to present stereo images as disclosed in [16]. A retro-reflective diffusing material consists of a retro-reflector sheet and a light diffusing sheet which diffuses light in one direction much more than the other directions. A retro-reflector reflects incident light back to the source. If a projector projects image onto a retro-reflector, retro-reflector forms an exit pupil at the same position as the projection lens. In order to see the projected

image, the viewer must look through the created exit pupil, but it is impossible for two objects, eye of the viewer and projection lens, to occupy same position in space. By placing a 1D diffuser before the retro-reflector, exit pupil is expanded in the vertical direction. Thus, anyone looks through vertically expanded exit pupil, called vertical viewing slit, can see the projected image. By placing multiple projectors horizontally apart from each other, as in [17], or by moving two projectors according to the position of the viewer [18], viewer can perceive 3D in a comfortable viewing area.

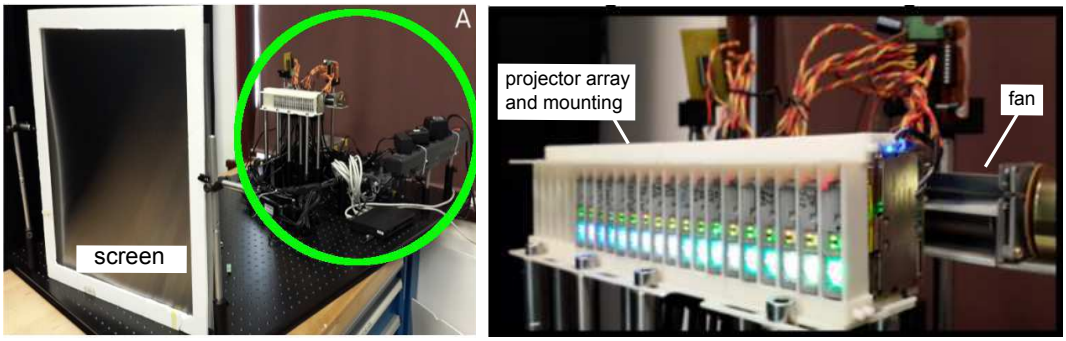

(a) (b)

Figure 2.5: a) Photographs showing a front view of the overall prototype consisting of 18 projectors, 3 mobile computers, and a 1D diffuser. b) Close-look at projector array circled in 2.5a.

2.5 Modular Multi-view Autostereoscopic Display using MEMS Projector Array

A good example of creating fixed viewing slits is Modular Multi-view Autostereoscopic Display developed in our group [19]. In this display, an array of 18 Microvision Inc. MEMS pico-projectors, a 1D diffuser with 40^o of diffusing angle, a pupil tracker and 3 mobile computational units are used **??**.

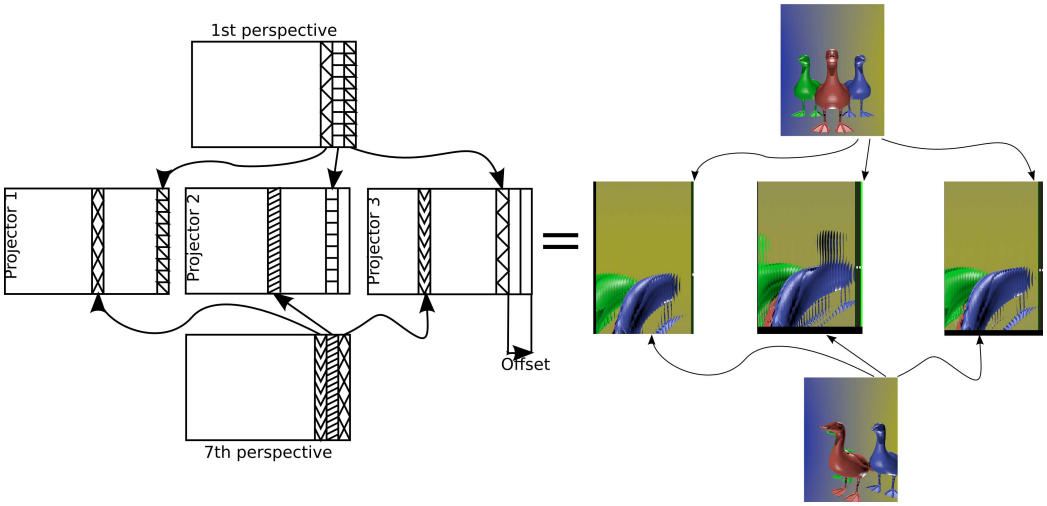

Figure 2.6: Content creation. For simplicity, only two perspective images and three projectors are shown.

Each projector in the projector array projects specially created different images to the 1D diffuser. Each of these specially created images contains different portions from different perspectives as seen in 2.6. A viewer looking through the vertical axis light dffuser screen sees one slit-shaped portion of this projected image. This portion of projected image is actually one portion from a specific perspective. The same viewer sees another portion of the same specific perspective from another projector. When all portions of this specific perspective is summed up together by all projectors in the projector array, the viewer sees a complete image of this specific perspective.

Chapter 3

PROPOSED DISPLAY

In this chapter, the methodology of the proposed autostereoscopic display, the characterization of the display and the constructed prototype with the quality measurements will be presented.

3.1 System Design

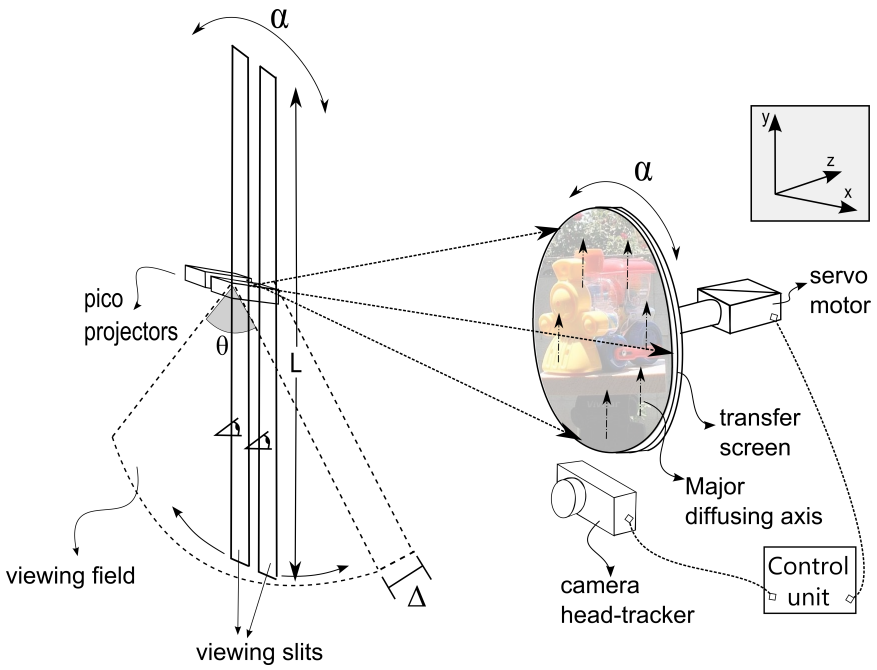

Figure 3.1: System sketch showing the elements and the created viewing field of the display.

The system sketch shown in Fig. 3.1 shows two pico projectors, a rotating transfer screen, an pupil-tracker unit, and a control unit. The stereo content is projected onto the transfer screen by two pico projectors which are placed horizontally apart from

each other by average human interpupillary distance (IPD), 63 mm. Each projector is assigned to one eye of the viewer. One projector projects the content for the right eye perspective and the other projects the content for the left eye perspective. On the plane of projectors, as shown in Fig. 3.1, the transfer screen creates two viewing slits, each of which is parallel to the major diffusing axis of the 1D diffuser, and crosses over the position of corresponding pico projector's micro electromechanical system (MEMS) based scanner. Each viewing slit contains the image content projected by the corresponding pico projector. The creation of viewing slits by using a retroreflective diffuser screen, as transfer screen, will be explained in section 3.1.1. A viewer, who is standing in the plane of pico projector and looks through the viewing slits, perceives stereo images.

In order to change the position of viewing slits according to the position of viewer's eyes, a pupil-tracker tracks the position of the viewer's pupils and sends the position information to the control unit. According to the position information, a motor rotates the transfer screen in-plane such that viewing slits dynamically follow the viewer's pupils in a large viewing field, as depicted in Fig. 3.1.

3.1.1 Formation of Viewing Slits

In order to understand the proposed method, one must know how an exit pupil, so called viewing slit is formed by a transfer screen, and what properties it has. Thus, in this section, the formation of viewing slits by the transfer screen will be explained. In the next section, the proposed method to change the position of viewing slits according to the viewer's position will be explained.

Autostereoscopic displays control light path such that they create viewing slits, through which different perspectives of the stereo image are observed, in different spatial positions. There are several different ways to control light path for autostereoscopic displays. One of them is relaying the projected image onto a slit shaped exit pupil, by a transfer screen which both diffuses light in a single axis and images at the same time. The transfer screen examples have been mentioned in Chapter 2. The transfer

screen can be thought as a special imaging system which consists of a 1D diffuser and an imaging lens.

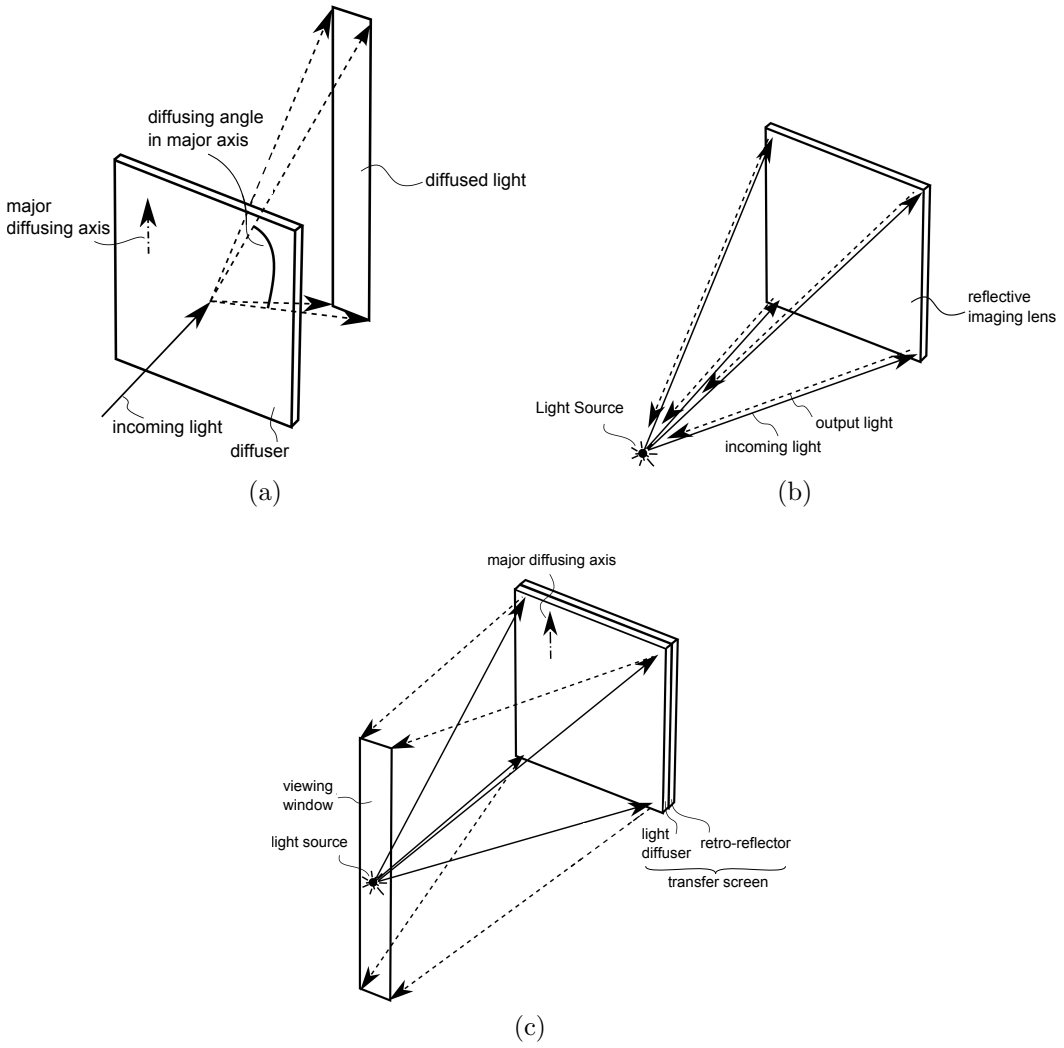

Figure 3.2: Working principle of a transfer screen (a) The effect of 1D diffuser on incident light (b) Imaging with reflective imaging lens such as retro-reflector (c) Formation of slit shaped viewing slit using transfer screen, consists of light diffuser and reflective imaging lens.

Figure 3.2a illustrates the effect of a 1D diffuser on an incident light ray. The 1D diffuser is characterized by diffusing angle in major axis, and diffusing angle in minor axis. Since the diffusing angle in major axis is much greater than the diffusing angle in minor axis for a 1D diffuser, it diffuses light in major diffusing axis much more than

its orthogonal axis, minor diffusing axis. Thus, when incident light ray passes through the 1D diffuser, the output light rays are diffused in line shape, and the diffused light is parallel to the major diffusing axis of the 1D diffuser.

Figure 3.2b illustrates the imaging of a light source by a reflective imaging lens. In the illustration, the reflective imaging lens does one to one imaging, thus the light source and its image are at the same spatial position. In Figure 3.2b, the image of light source is not illustrated for the sake of simplicity. A retro-reflector is an example for a one-to-one reflective imaging lens.

Figure 3.2c illustrates the formation of viewing slit by a transfer screen. The transfer screen consists of a 1D diffuser, illustrated in Figure 3.2a and a reflective imaging lens , illustrated in Figure 3.2b. Light rays from the light source hits on the transfer screen, and transfer screen forms a slit shaped viewing slit in which lights from light source are collected. As seen in Figure 3.2c, the created viewing slit has two important properties; 1) It is parallel to the major diffusing axis of transfer screen, 2) It is anchored by its center to a virtual anchor point, which is the spatial position of image of light source. The importance of these properties will be explained in the next section. Since imaging lens in the transfer screen does one-to-one imaging, the image of light source and light source itself are in the same spatial positions.

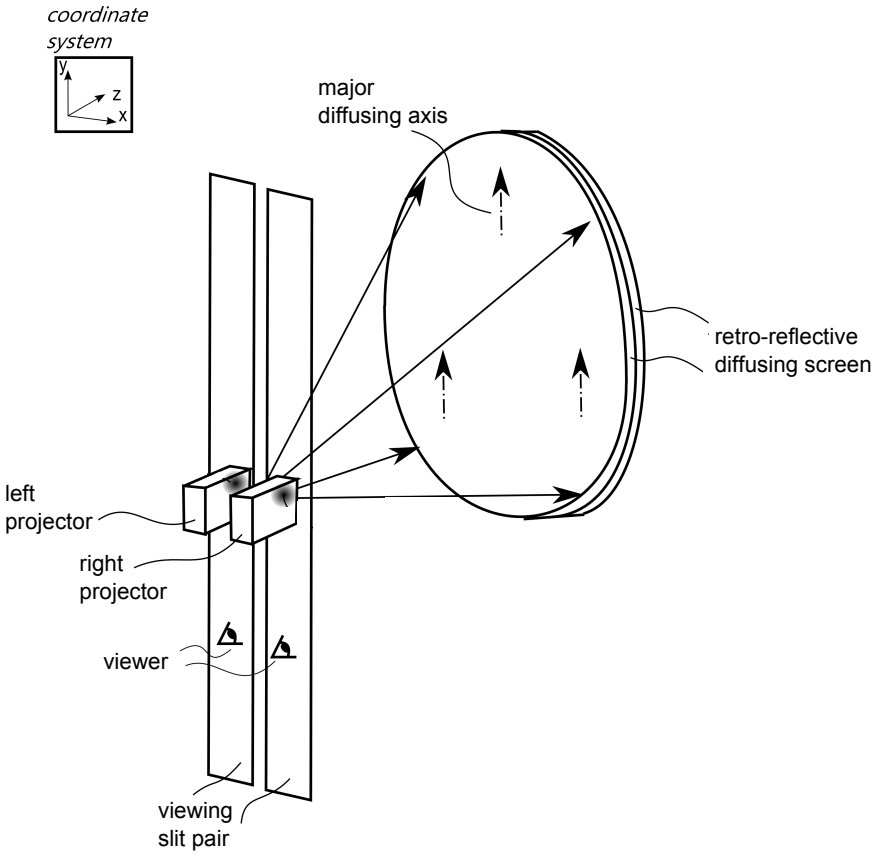

Figure 3.3: The formation of viewing slit pair through which viewer perceives the stereo image without need of any special glasses.

Figure 3.3 illustrates the formation of viewing slit pair, through which stereo image can be perceived. Instead of light source depicted in Figure 3.2a and 3.2b, two projectors are used and placed apart from each other by an average human interpupillary distance, (IPD). One of projectors, right eye projector projects right eye image of stereo image pair, and the other, left eye projector projects left eye image of stereo image pair onto the transfer screen. The transfer screen forms two viewing slits, right and left eye viewing slits through which right and left eye image of stereo image pair are presented, respectively. Since the projectors are placed apart from each other by interpupillary distance, the viewer's eyes can fit into viewing slits correctly.

3.1.2 Changing Position of Viewing Slits

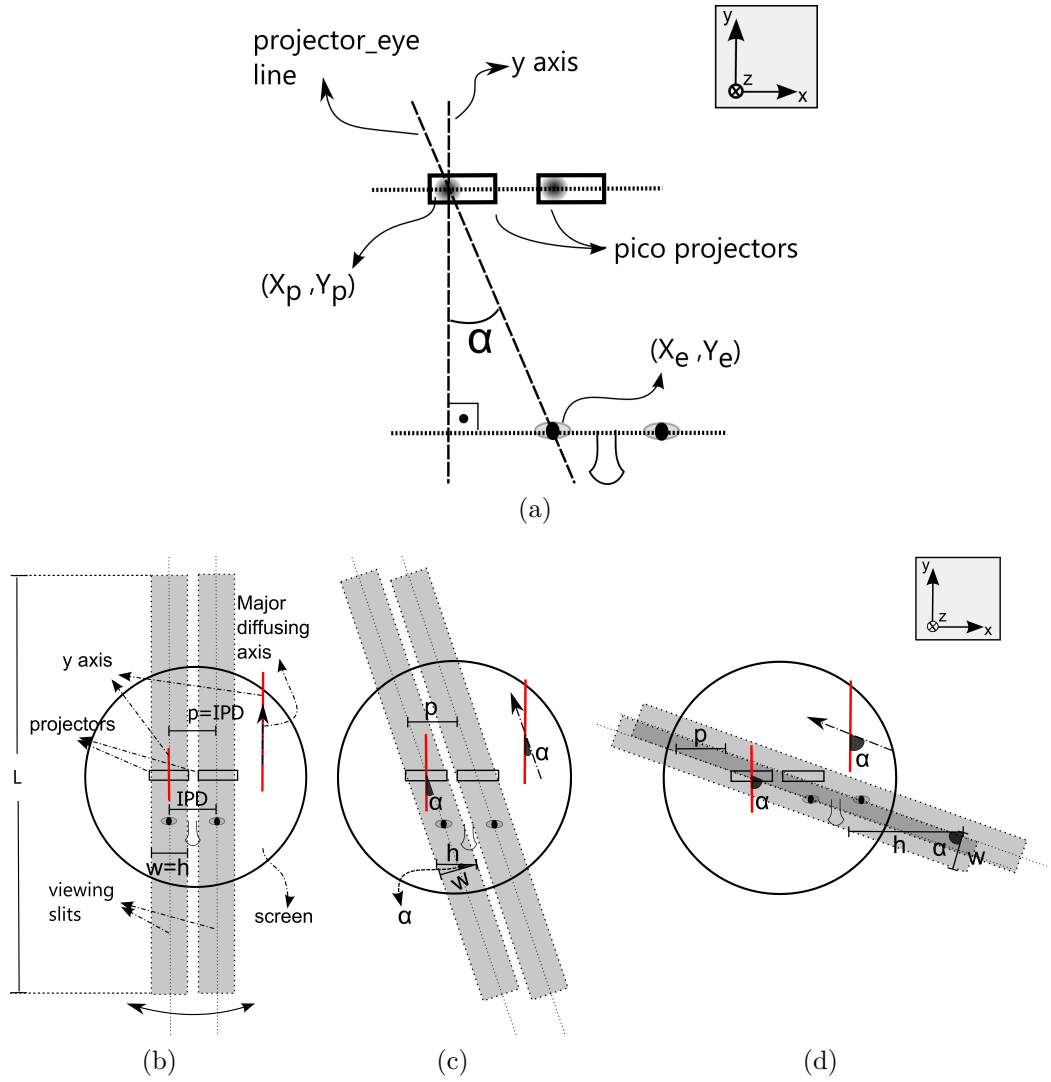

Figure 3.4: Viewing slits for different orientations of the transfer screen. (a) Relative angular position of viewer's eyes with respect to projectors (b) Rotation of transfer screen by 0^o of α and $w < 2 \times IPD$, thus $h = w < 2 \times IPD$ (c) Rotation of transfer screen by small α, thus $w < h < 2 \times IPD$ (d) Rotation of transfer screen by large α, thus $h > 2 \times IPD > w$, and there is crosstalk between viewing slits.

Figure 3.4b is the front view of the system, illustrated in Figure 3.3, when the major diffusing axis of transfer screen is parallel to the y axis. Since two projectors are placed apart from each other by interpupillary distance, d, the distance between the

center line of viewing slits is interpupillary distance, d. Thus, eyes of the viewer fit into viewing slits, and viewer perceives stereo images, as long as viewer's eyes are aligned on an axis which is parallel to the axis of projectors.

$$\alpha = arctan(\frac{X_e - X_p}{Y_e - Y_p}) \tag{3.1}$$

When the viewer changes its position, the pupil-tracker unit locates eyes of the viewer, and feeds the position information of viewers eyes to the control electronics. The control electronics calculates the angular position of eyes relative to the position of projectors, as illustrated in Figure 3.4a. The positions of projectors (X_p,Y_p) are always fixed and they are known by the control electronics. Since the positions of viewers eyes (X_e,Y_e) and the position of projectors (X_p,Y_p) are known by the control electronics, the control electronics calculates the angular position of the viewer which is the angle, α, between reference axis and projector-eye line as in Equation 3.1. The reference axis is the axis which is perpendicular to the axis of projectors, and the projector-eye line is the axis on which one of viewers eyes and the corresponding projector are aligned.

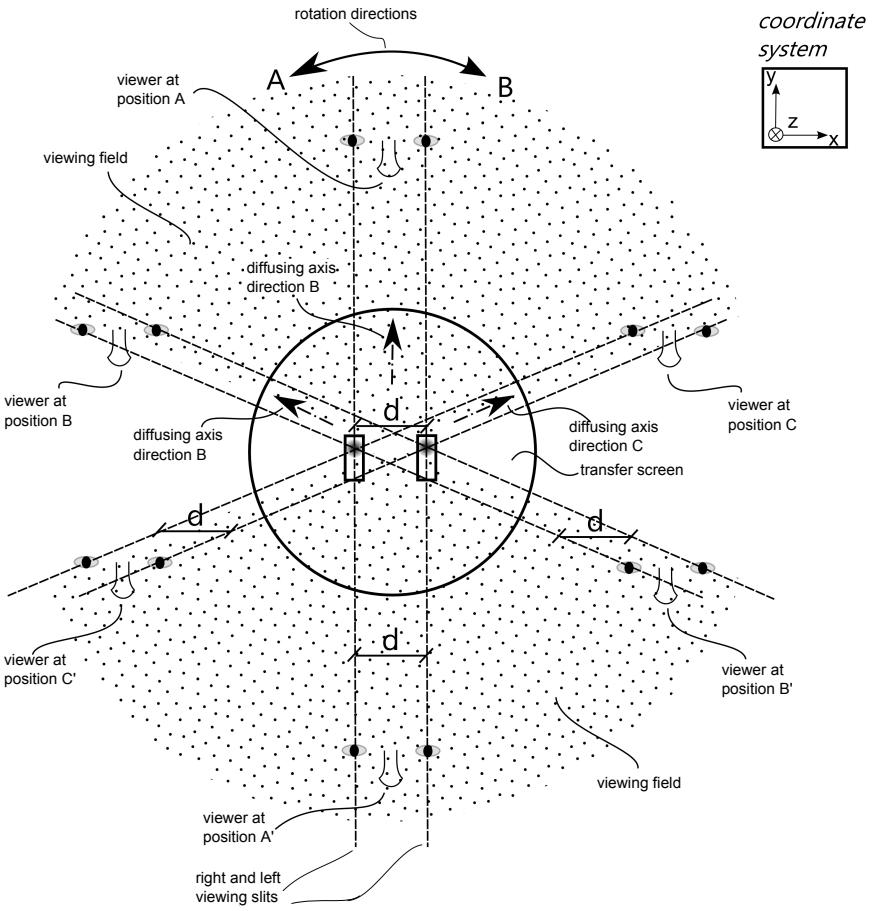

Figure 3.5: Illustration of 6 different cases for the position of viewer and corresponding positions of viewing slits. For the sake of simplicity, only center lines of the viewing slits are shown.

After the calculation of angle, α, the motor rotates the transfer screen around its center, such that the angle between major diffusing axis of transfer screen and reference axis is also angle of α, as in Figure 3.4d. Since the viewing slit is parallel to the major diffusing axis of transfer screen as explained in the previous section, right and left eye viewing slits are also rotated and formed on the spatial position of right and left eye of viewer, respectively. The aformentioned procedure are performed in real time, and viewing slits dynamically track the viewer in a large viewing field, as depicted in Figure 3.5. The motion of the viewing slits is analogous to the in-plane rotation of a beam around an anchor point. The MEMS scanner of the pico projector is the anchor point of the corresponding viewing slit, as mentioned in the previous

section. Thus, rotation of transfer screen doesn't change the interpupillary distance between the center lines of viewing slits along the axis of projectors and eyes of the viewer can look through viewing slits.

3.1.3 Characterization of Display

Table 3.1: Definitions of Symbols

	Parameter	Symbol
Prototype Parameters	Projection Distance	d
	Projection Angle	β
	Screen size	s
	Diffusing angle in major axis (FWHM)	ϕ
	Diffusing angle in minor axis (FWHM)	ψ
	Distance between two projectors	p
	Diameter of projector's MEMS scanner	d_p
	Interpupillary Distance	IPD
Viewing Slits Parameters	Distance between slits	p
	Actual width	w
	Horizontal width	h
	Rotation angle	α
	Length	L
	Maximum rotation angle	θ
	Depth	Δ

The viewing field of the proposed autostereoscopic display technique is characterized by the length, L, depth, Δ, and the maximum rotation angle, θ, of viewing slits, as depicted in Fig. 3.1. For the proposed technique, the viewing field has been defined as the three-dimensional space in which the crosstalk value of the display is low enough to perceive stereo images.

$$L = 2 \times d \times tan(\phi/2) \tag{3.2}$$

The length, L, of viewing slits characterizes the luminance of the display across the projector plane. It is determined by the projection distance, d, and diffusing angle, ϕ, of 1D diffuser in major axis, as in Eq. 3.2. As the viewer moves away from the

center of the viewing slit, which is the position of the pico projector, the luminance of the display decreases, according to the diffusing properties of the diffuser. If the diffusing angle, ϕ, is expressed as full-width-at-half-maximum (FWHM) value, then the luminance of the display is less than 50% of the maximum luminance beyond the length, L, of viewing slits.

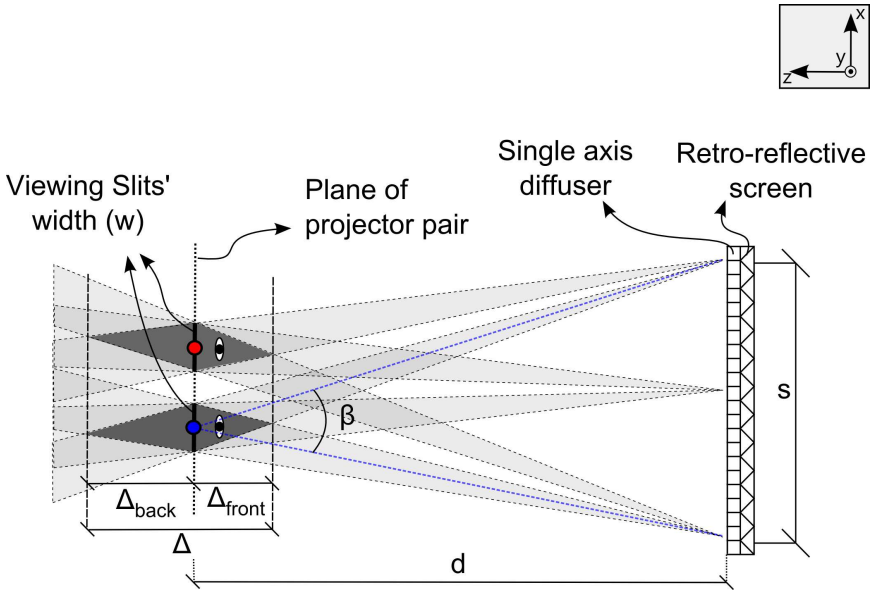

Figure 3.6: Top view of the system showing depth of viewing slits

$$\frac{s}{w} = \frac{d - \Delta_{front}}{\Delta_{front}} = \frac{d + \Delta_{back}}{\Delta_{back}} \tag{3.3}$$

$$\Delta = \Delta_{front} + \Delta_{back} = \frac{d}{\frac{s}{w} + 1} + \frac{d}{\frac{s}{w} - 1} \tag{3.4}$$

The depth, Δ, of the viewing slits characterizes the luminance of the display along the projection axis. As the viewer moves away from the projector plane along the projection axis, the luminance decreases at the edges of the transfer screen. Figure 3.6 illustrates a top view of the proposed system. In Fig. 3.6, the projection angle of the projector is shown as β, projectors to screen distance is shown as d, the width of viewing slit is shown as ω, and the depth of viewing slits is shown as Δ. By using

the triangle similarity expressed in Eq. 3.3, the depth, Δ, of viewing slits can be calculated as in Eq. 3.4. If the width, ω is FWHM value, the luminance at the edges of the transfer screen is less than 50% of the maximum luminance beyond the depth, Δ, of viewing slits.

$$h = \frac{w}{cos(\alpha)} \tag{3.5}$$

$$h < 2 \times IPD \tag{3.6}$$

$$\alpha < \theta = arccos(\frac{w}{2 \times IPD}) \tag{3.7}$$

The maximum rotation angle, Θ, of the viewing slits is the rotation angle, α, beyond which the horizontal width of the viewing slits, h, is larger than $2 \times IPD$, as in Fig. 3.4d, and crosstalk results in inseparable stereo images. The horizontal width of viewing slits, h, is the full-width-at-zero-intensity (FWZI) width of viewing slits along the horizontal axis, x-axis. In order to avoid crosstalk between stereo images, following two conditions must be satisfied in the proposed system design; (1) the horizontal distance between viewing slits, p, must be equal to interpupillary distance of the viewer, IPD, and (2) the horizontal width of viewing slits, h, must be smaller than $2 \times IPD$, as in Figs. 3.4b and 3.4c.

The transfer screen does one-to-one imaging to form exit pupils of pico projectors. Placing two projectors horizontally apart from each other by IPD makes the horizontal distance between viewing slits, p, equal to the interpupillary distance of the viewer, IPD. Thus, the aforementioned first condition to avoid crosstalk is satisfied, as long as the viewer's eyes are aligned along the horizontal axis.

The horizontal width of viewing slits, h, increases with the increase in rotation angle, α, of viewing slits, as seen in Figs. 3.4b-3.4d. The relationship between the horizontal width, h, and rotation angle, α, of viewing slits is stated in Eq. 3.5, where ω is the actual width of viewing slits. It is the FWZI width of the viewing slit, which

is measured across the viewing slit at right angles of its length. It is a fixed system parameter which is proportional to the projection distance, d, the diffusing angle of 1D diffuser in minor axis, ψ, and the diameter of MEMS scanner of projector, d_p. By placing Eq. 3.5 into Eq. 3.6, the second condition to avoid crosstalk, stated in Eq. 3.6, can be restated as in Eq. 3.7. Equation 3.7 implies that there is a maximum rotation angle, α, of viewing slits, beyond which crosstalk results in inseparable stereo images.

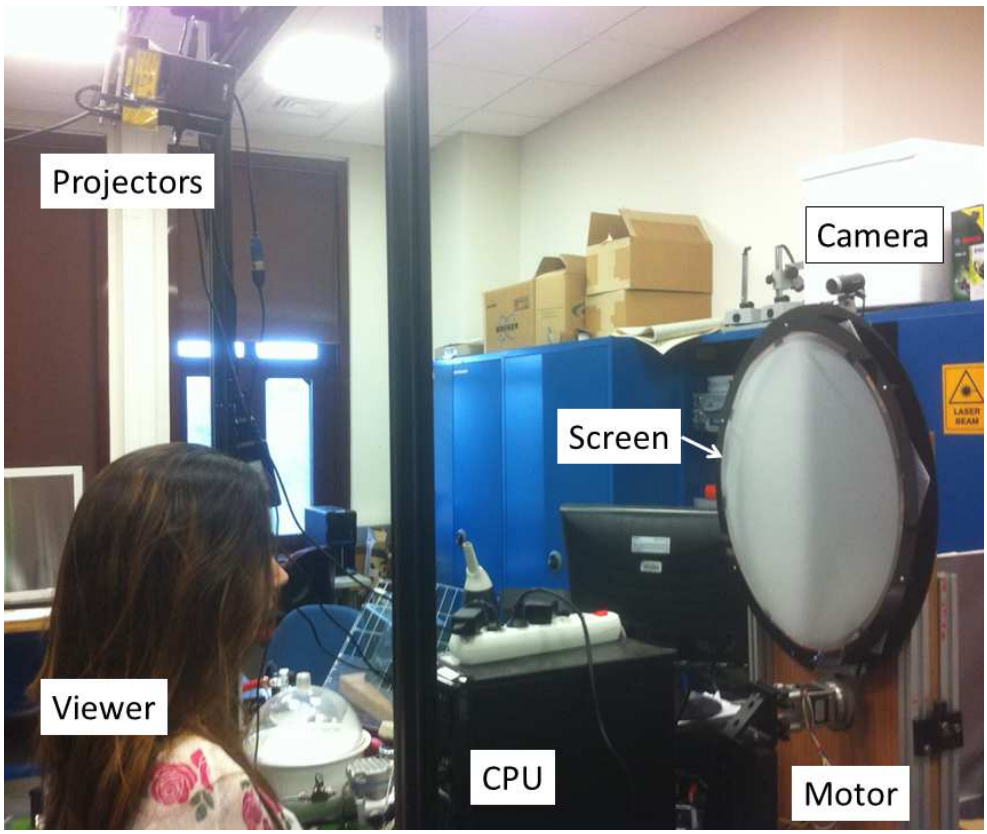

Figure 3.7: The realised prototype.

3.2 Constructed Prototype

A prototype was realised to demonstrate the capabilities of the proposed technique. The prototype consists of two MEMS based laser pico projectors from Microvision, Inc. [20], a retro-reflective diffuser screen as a transfer screen [16], a pupil-tracker unit [21], a rotating mechanism which rotates the transfer screen around its center,

and a personal computer. Figure 3.7 a shows a photograph of the realised prototype.

Table 3.2: Prototype Parameters

Parameter	Symbol	Value
Projection Distance	d	1180 mm
Projection Angle	β	28.4^o
Screen size	s	600 mm
Diffusing angle in major axis (FWHM)	ϕ	40^o
Diffusing angle in minor axis (FWHM)	ψ	0.2^o
Distance between two projectors	p	63 mm
Diameter of projector MEMS scanner	d_p	1 mm
Diameter of eye pupil	d_{eye}	2 $mm - 8$ mm
Interpupillary Distance	IPD	63 mm

3.2.1 Mems Based Laser scanning Pico Projectors

Projectors used in the prototype are MEMS based laser scanning pico projectors from Microvision, Inc. [20]. The device contains red, green, and blue color lasers which are all linear polarized with polarization of green is perpendicular to the polarizations of red and blue. The light from all three lasers is combined and scanned by a MEMS scanner in two axes using a raster scan pattern. By doing so, the projector forms an image on the projected surface, as in fig 3.8a.

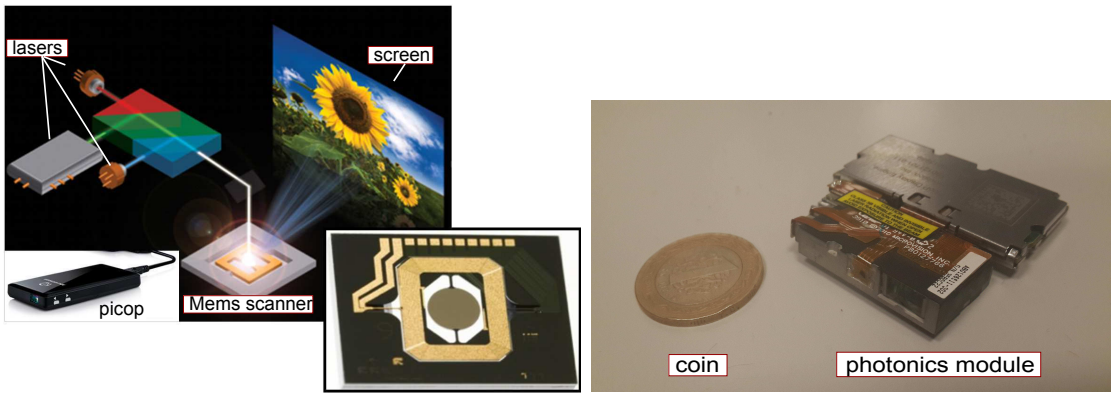

(a) (b)

Figure 3.8: a) Left picture shows the pico projector and a sketch of interior photonics module. Right bottom picture is a photo of MEMS scanner. b) Photonics module of a pico projector.

Since there is no lenses inside the projector and lasers are collimated, the projected image is always on focus. Thus, a focus free projector gives freedom to scale the display system. The photonics module consisting of lasers is shown in the fig 3.8b.

Pico-projectors have been used in many different applications and settings. One of them is Portable 3D Laser Projector Using Mixed Polarization Technique which is developed in our group, [O1]. Polarization difference between lasers of pico-projector, and Mems technology in the pico-projector allow us to present full resolution 3D image with only a single pico-projector.

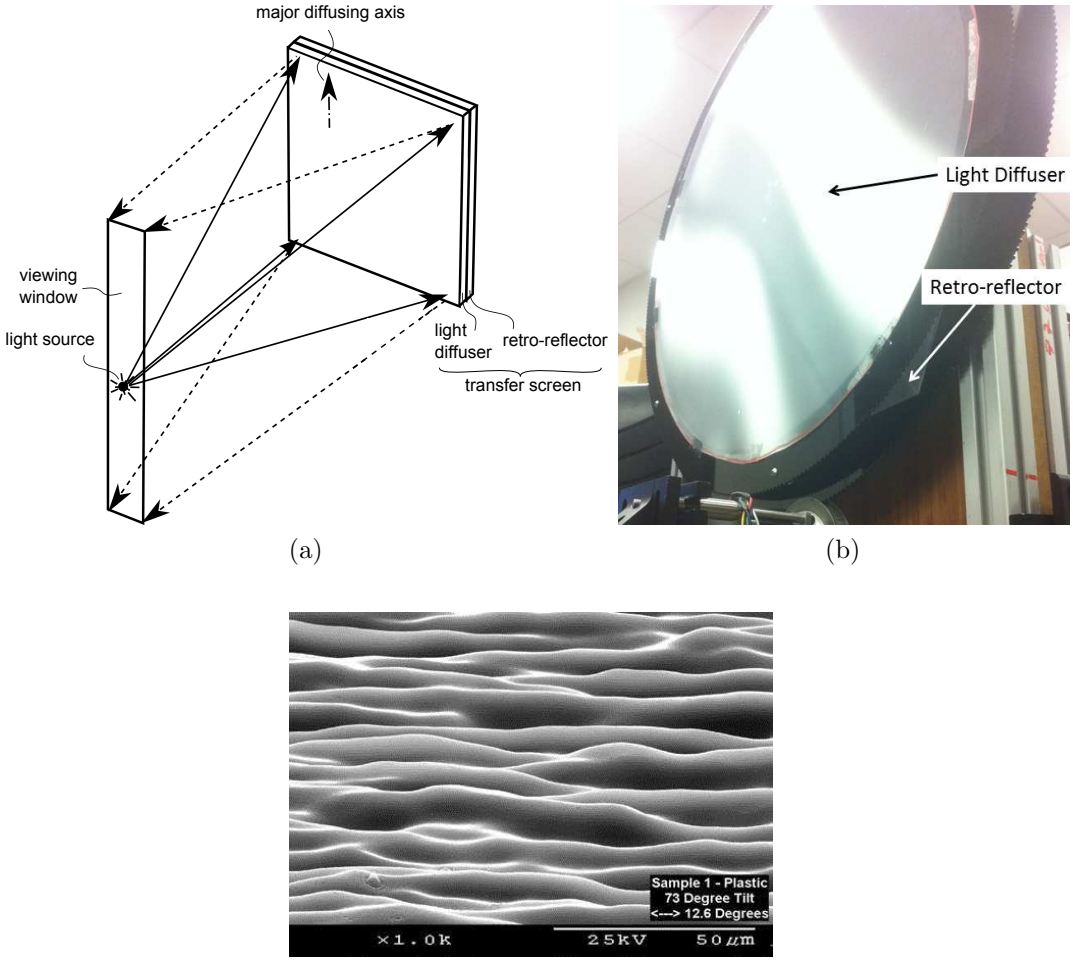

(a) (b)

(c)

Figure 3.9: a) The sketch of retro-reflective diffusing screen b) the picture of retro-reflective diffusing screen c) SEM picture of aperiodic single axis diffuser from Luminit, LLC.

3.2.2 Retro-reflective Diffusing Screen

The transfer screen is a layered composition of a retro-reflective sheet [15] from Reflexite [16], and a 1D diffuser (large diffusing angle in major axis and small diffusing angle in the perpendicular minor axis), as seen in fig 3.9. Two different types of 1D diffuser have been tested as the diffuser layer of the transfer screen. Diffuser 1 is a randomly patterned aperiodic diffuser from Luminit, LLC [17] with FWHM diffusing angle, ϕ, of 40^o in major axis, and, ψ of 0.2^o in minor axis. Diffuser 2 is a conventional periodic

diffuser with FWHM diffusing angle, ϕ, of 20^o in major axis, and, ψ of $\sim 0^o$ in minor axis. The retro-reflector sheet is a high fill factor corner cube retro-reflector array with 0.254 mm pitch size and it is hexagonal with 600 mm diagonal length. As the screen size is equal to the retro-reflector sheet size, it can be enlarged using an improved mechanical design to support a larger screen. All prototype parameters are presented in Table 3.2.

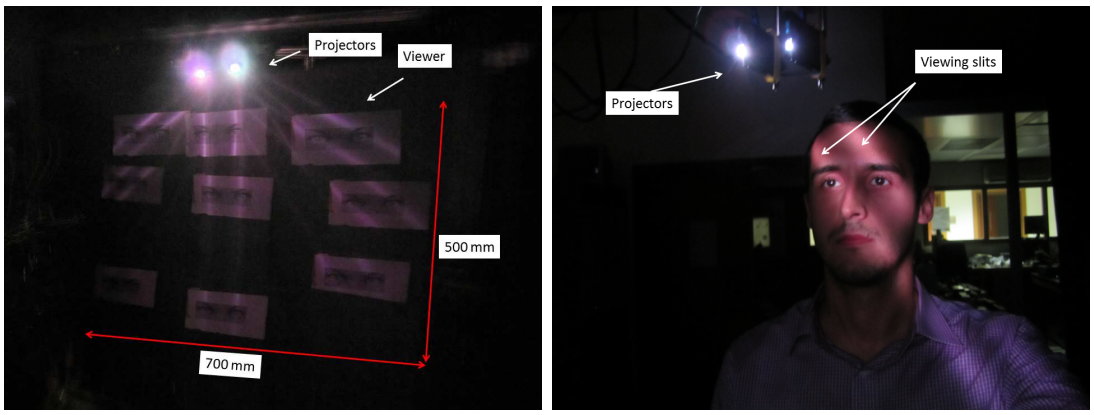

(a) (b)

Figure 3.10: (a) Created viewing slits at different rotation angles: 9 shots are superimposed in order to create the photograph. The two bright spots in the photograph are pico projectors. (b) A sample picture of viewer, showing viewing slits on his eyes' position.

3.2.3 Created Viewing Field

The creation of viewing field by rotating the transfer screen is explained in chapter 3. As mentioned in chapter 3, it is enough to rotate only single axis diffuser in order to create dynamic viewing slits in the viewing field. However, in the prototype, rotating mechanism rotates both retro-reflector sheet and the 1D diffuser which makes the realization of the prototype easier. The created viewing field is illustrated in Fig. 3.10a by taking pictures of viewer space for different rotation angles of viewing slits. Figure 3.10b shows a sample picture of viewer while viewing slits appear on his eyes' position.

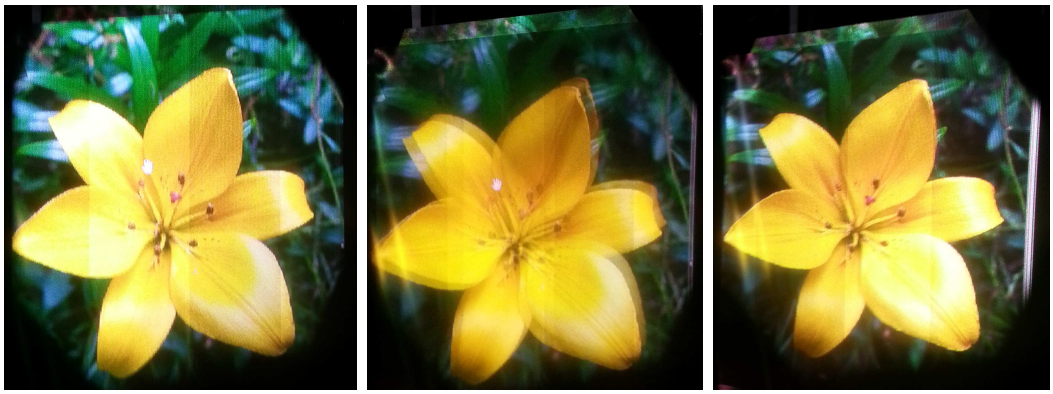

(a) (b) (c)

Figure 3.11: Screen shots taken from different viewing positions: (a) left eye, (b) between the two eyes, and (c) right eye.

Specular reflections create two bright lines across the transfer screen, which result in double image along the bright lines. The specular reflections can be eliminated by anti-reflection (AR) coating surfaces, or by tilting the transfer screen around the vertical axis, y-axis. In the prototype, display screen has been tilted by 5^o around the vertical axis, so specular reflections are not observed on the transfer screen. Fig. 3.11a is a picture of the screen taken from the left eye viewing slit. Fig. 3.11b is a picture of the screen taken between left and right eye viewing slits, thus both right and left eye images are observed. Fig. 3.11c is a picture of the screen taken from the right eye viewing slit.

Table 3.3: Mechanical Design Parameters

Parameter	Design 1	Design 2	Formula
screen mass	2 kg	1 kg	m_d
screen radius	0.3 m	0.3 m	r_d
screen inertia	0.09 kgm^2	0.045 kgm^2	$I = \frac{1}{2} \times m_d \times r_d^2$
angular velocity	0.5π rad/sec	0.5π rad/sec	w
acceleration time	0.2 sec	0.2 sec	t
angular acceleration	15.7 rad/sec^2	15.7 rad/sec^2	$\alpha = \frac{\Delta w}{\Delta t}$
screen torque	1.41 Nm	0.7 Nm	$\tau_s = I \times \alpha$
gear ratio	1:1	1:4	$gear_m/gear_s$
motor torque	0.94 Nm	0.9 Nm	$\tau_m = F \times d$

3.2.4 Mechanical Analysis of Screen Rotation

In the proposed display, screen rotation is a key element of the system implementation. The angular speed and acceleration of the screen must be enough to track viewer movements without any latency. In order to do so, the system must produce enough torque and has an efficient power transmission between the motor and the screen. Minimum angular speed of the screen is determined such that viewing slits must travel between two edges of the viewing field in one second. Maximum rotation angle of the screen is approximately 45^o in one direction and angular distance between two edges of the viewing field is 90^o as it will be explained in 3.3. Thus, the screen must be rotated with an angular velocity of 0.5π rad/sec. Acceleration time of the screen is determined as 0.1 sec. In order to rotate screen with these specifications, two different mechanical design have been applied to the prototype and the overall screen weight has been improved during the thesis study. Mechanical design parameters can be found in table 3.3. In the next paragraphs, two design will be compared and discussed.

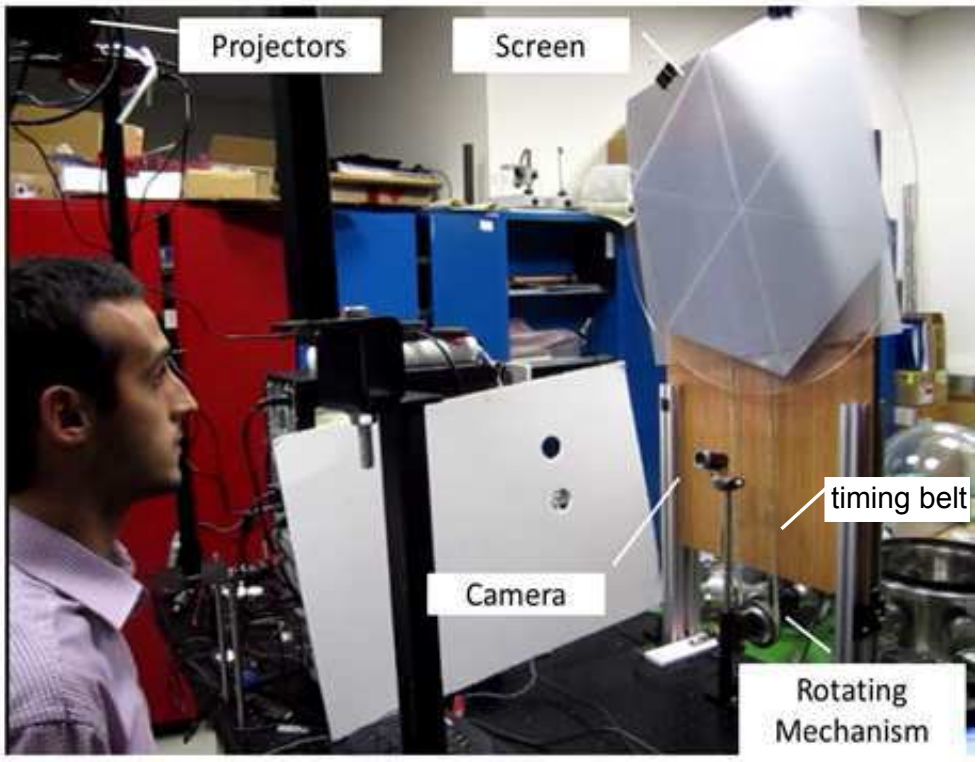

Figure 3.12: A picture of constructed prototype by using timing-belt system for power transmission.

3.2.4.1 Mechanical Design 1

Figure 3.12 is a picture of the prototype with the mechanical design 1. In the first mechanical design, a servo motor is used to rotate the screen. A gear with radius of 7.5 mm has been assembled to the servo motor. Another gear with the same radius of 7.5 mm has been produced by using a 3D printer and assembled onto the center of the back side of screen, fig. 3.13b. The servo motor has been connected to the screen via a timing-belt system with one-to-one gear ratio as seen in Fig. 3.13a. The screen is placed onto a roller bearing and able to rotate around its center.

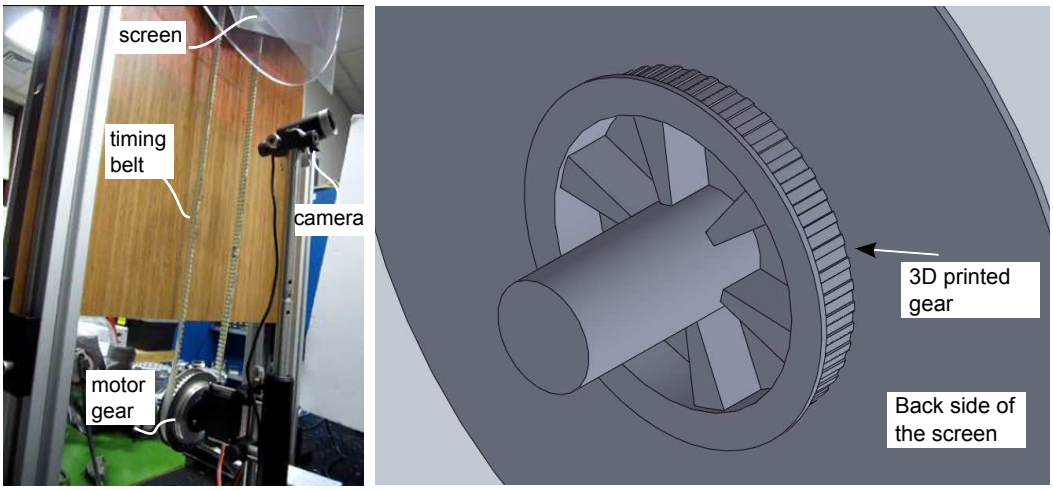

(a) (b)

Figure 3.13: a) Closer look at timing-belt system. b) 3D sketch of home-made gear

In the first mechanical design, the screen mass is 2 kg, and screen radius is 0.3 m. In order to rotate this screen with angular acceleration of 15.7 rad/sec^2, 1.41 Nm torque is needed as calculated in Table 3.3. The servo motor used in this design is a TowerPro MG995 servo motor with 0.94 $N.m$ holding torque. Since the gear ratio is 1:1 between the motor and the screen, the servo motor provides 0.94 $N.m$ to the screen. The provided torque is smaller than the needed screen torque with aforementioned speed configurations. Thus, we have applied a new mechanical design and decreased the weight of the screen with a new mounting.

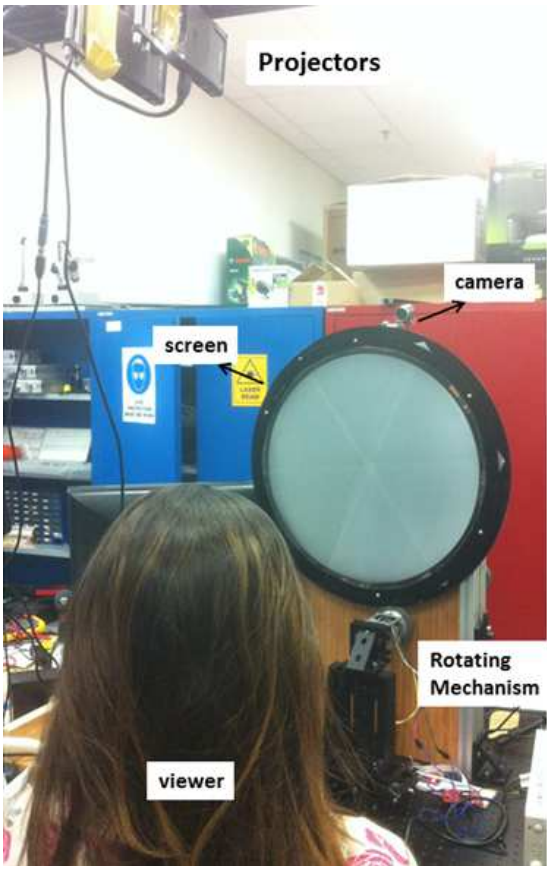

Figure 3.14: A picture of constructed prototype by using two-gear system for power transmission.

3.2.4.2 Mechanical Design 2

In mechanical design 2, instead of using a timing belt between the motor and the screen, a two-gear system has been implemented for torque transmission as seen in 3.14. The screen is placed onto a ring shaped disc with 0.3 m radius and it is made of 3 mm thick plexi glass material. The overall weight of the screen has been decreased to 1 kg. The circumference of the disc has been cut in toothed shaped as seen in 3.15. Thus, in the two gear system, one gear is the gear with 75 mm radius mounted onto the motor, the other gear is the screen itself with 300 mm radius and gear ratio is 1:4. By this implementation, a more efficient torque transmission has been achieved due to increase in gear ratio, Table 3.3, and lighter screen was obtained.

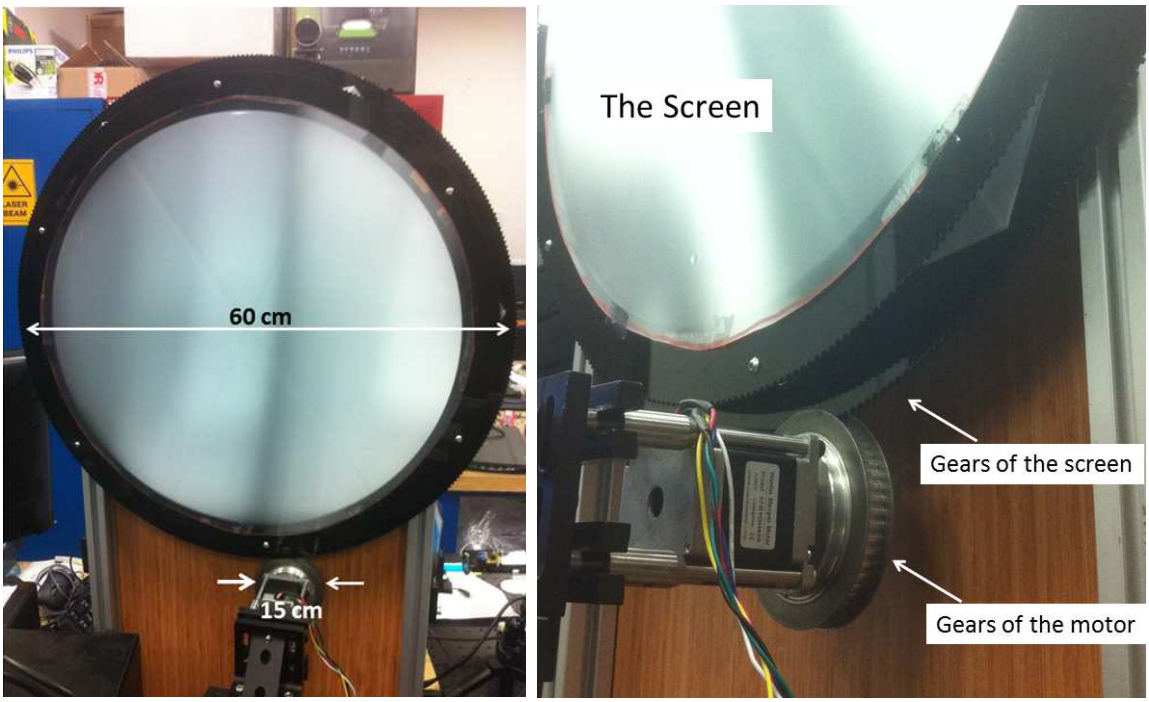

(a) (b)

Figure 3.15: a) The diameters of screen and motor gear. b) The produced gear-shaped back plate for the screen

In order to rotate new screen with angular acceleration of 15.7 rad/sec^2, 0.7 Nm torque is needed as calculated in Table 3.3. The step motor used in the prototype is Wantai 57BYGH420 which has holding torque of 0.9 $N.m$. Since the gear ratio is 1:4 between the motor and the screen, the step motor can provide 3.6 $N.m$ to the screen. The provided torque, 3.6 $N.m$, is much larger than the needed screen torque, 0.7 Nm. Thus, mechanical design 2 fulfill the needs of the screen rotation.

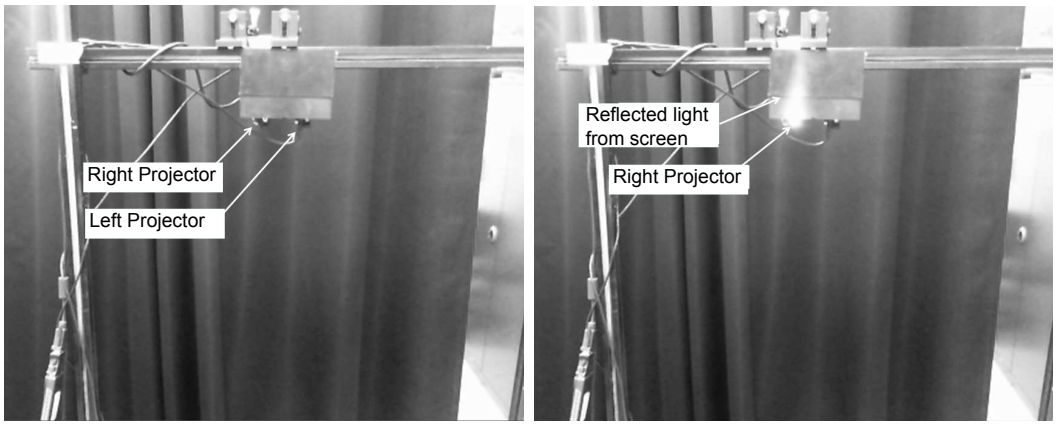

(a) (b)

Figure 3.16: a) Reference image taken from pupil-tracker camera. All projectors are off. b)Sample image. Right projector is on and left projector is off.

3.2.5 Pupil-Tracker and Camera-Projectors Calibration

Pupil tracking is a key element of the display since the rotation of the screen is synchronized with the position of the viewer. There are many different methods to find the position of viewer's pupils. In the prototype, an OpenCv script which utilizes the Haar Feature-based Cascade Classifiers is written and been used. Microsoft Lifecam 720p webcam is placed to a position where the camera can easily see the viewer and projectors. The image captured from the camera is fed into the CPU then CPU calculates the position of viewer's eyes by using the OpenCv script. In the proposed display, the important position is the relative position of viewer's eyes with respect to each projectors since the screen is rotated accordingly.

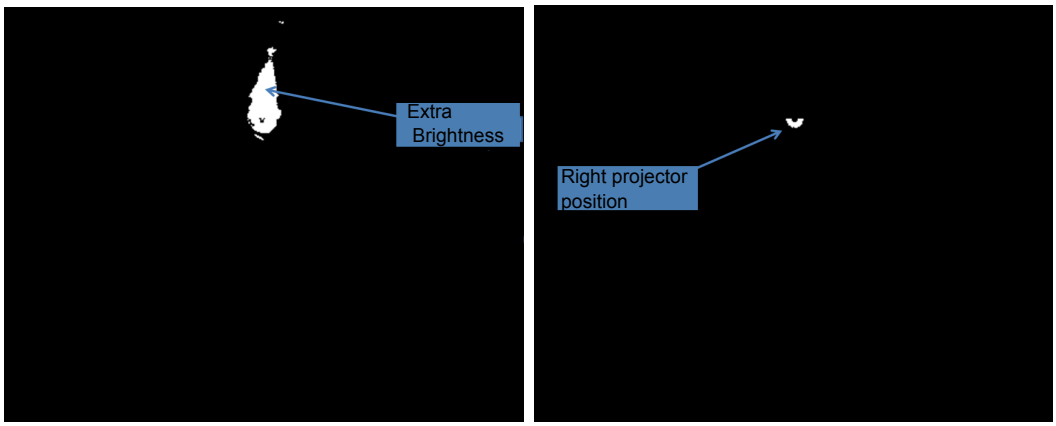

(a) (b)

Figure 3.17: a) Difference image between fig 3.16b and fig 3.16a with lower threshold value. b) Difference image with larger threshold value.

Since the prototype uses the relative position of viewer's eyes with respect to the projectors, the position of projectors must be known. Thus, each time prototype turns on, position of projectors must be calculated. In order to calculate the position of projectors, an OpenCv script is written which utilizes the image differencing method. The method uses the brightness difference between a reference image and sample image. When the prototype turns on, the camera captures a reference image which is captured when both projectors are off. The reference image is shown in fig 3.16a. Afterwards, sample image is captured when right projector projects a full white image, and left projector is off. The sample image is shown in fig 3.16b. The sample image is substracted from the reference image and a threshold is applied to the substracted image. The substracted image can be seen in fig 3.17a. The largest difference between two images are on the exact position of projector, thus threshold value is increased and applied to the substracted image. A new image is obtained and shown in fig 3.17b. As seen from the fig. 3.17b, the position of the right projector is found in terms of pixels value.

The same procedure that is applied for right projector is applied for the left projector and the position of left projector in terms of pixel values is found, too. By

placing position of projectors, (X_p, Y_p), and position of viewer's pupils, (X_e, Y_e), which are detected by the pupil-tracker into equ 3.1, angular position of viewer's pupils is found. By doing so, angular position of the viewer is obtained in real time, and the screen is rotated accordingly as explained in 3.1.2.

3.3 Measurements and Results

As a quality measure, a crosstalk analysis of the realized prototype for both diffusers was conducted. The crosstalk has been quantized by Eq. 3.8, where *leakage* is the maximum luminance of light that leaks from unintended channel to the intended channel, and 'signal' is maximum luminance of the intended channel, [22].

$$crosstalk(\%) = \frac{leakage}{signal} \times 100 \tag{3.8}$$

Thus, two luminance measurements of the screen are taken from each eye's position to calculate the crosstalk value of the corresponding eye. In the conducted experiments, only crosstalk values for the left eye has been measured, since the system is approximately symmetrical. For the first luminance measurement, which determines the leakage, full black image is projected by left-eye projector, and full white image is projected by right-eye projector. For the second measurement, which determines the signal, images for the first measurement are swapped. Luminance values have been measured by a calibrated camera from Radiant Imaging, which takes photometrically weighted photographs, and inserted into Eq. 3.8. By repeating the explained procedure above for different positions of camera in viewer's space, and interpolating the measured values; crosstalk, and luminance maps of viewer's space have been obtained for both transfer screen with diffuser 1, and transfer screen with diffuser 2.

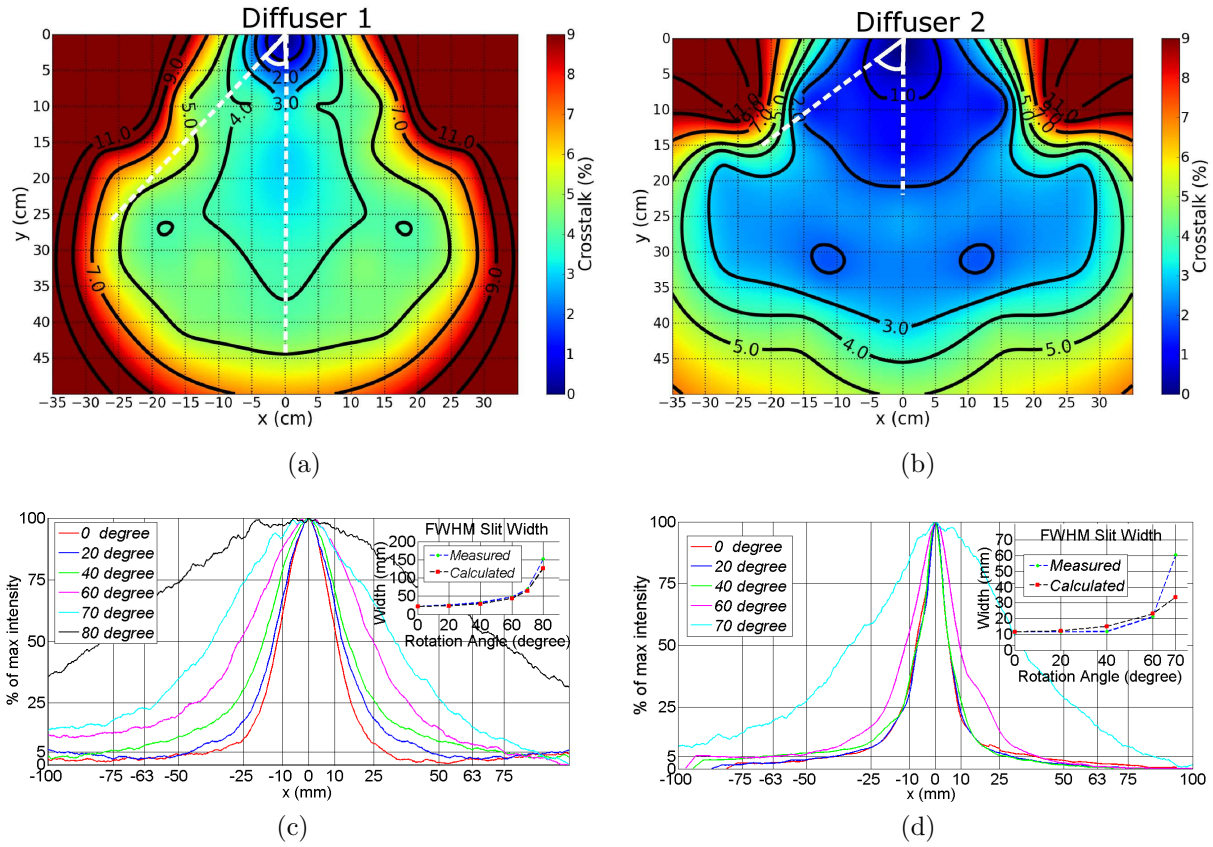

Figure 3.18: (a) and (b) Interpolated crosstalk maps of viewer's space at the projector plane for diffusers I and II. (c) and (d) Horizontal cross-sections of viewing slits for different rotation angle, a for diffusers I and II.

Figure 3.18a is the obtained crosstalk map of the viewer's space in projector plane for screen with diffuser 1. According to [23], crosstalk should be less than 5 % in order to prevent reduced viewing comfort in half of population. Thus the maximum rotation angle, θ, of viewing slits is 46^o, beyond which the crosstalk is more than 5 %, and results in inseparable stereo images. Figure 3.18c illustrates the horizontal cross-section of viewing slits for different rotation angles. The actual width, w, of viewing slits, which is the full width at 5 % of maximum intensity, for 0^o of rotation, is 75 mm. By placing the actual width, w, of viewing slit into Eq. 3.7, the maximum rotation angle, θ, of viewing slits is calculated as 53^0, which validates the experimental result of 46^o.

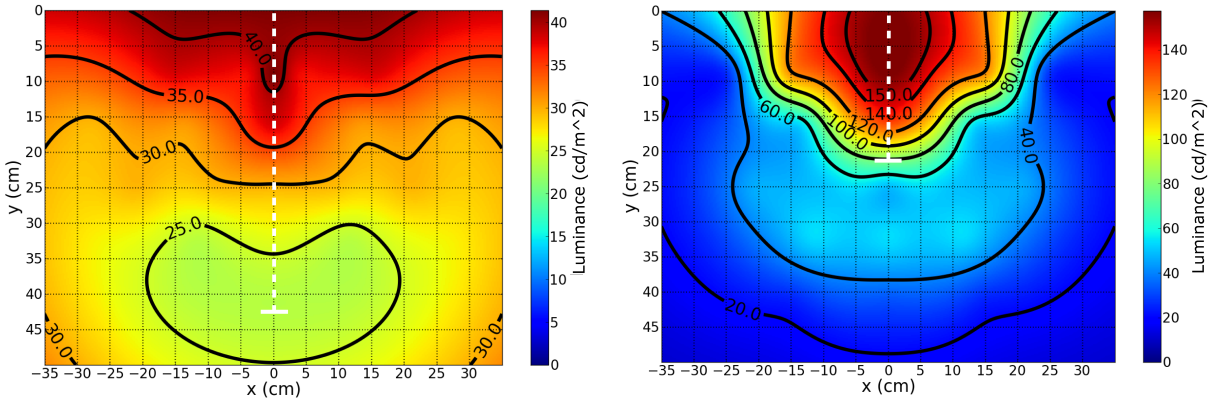

(a) (b)

Figure 3.19: (a) and (b) Interpolated luminance map of viewer's space at the projector plane for diffuser 1 and 2.

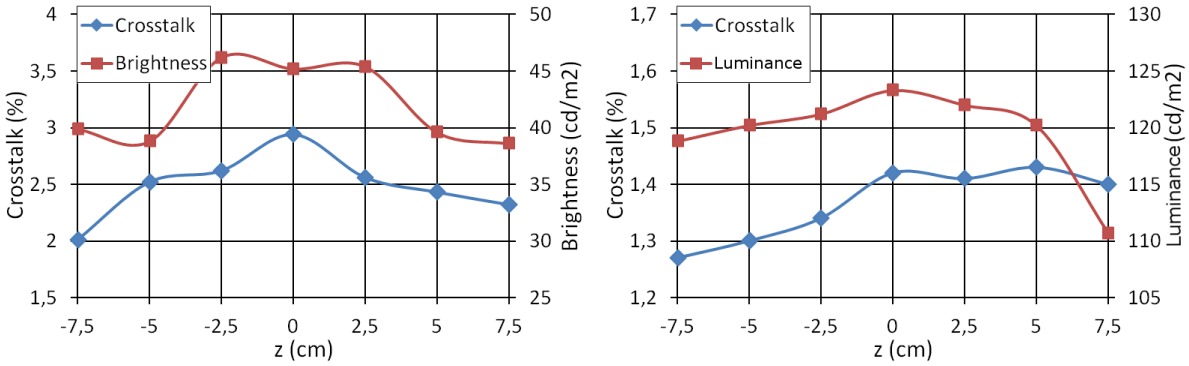

(a) (b)

Figure 3.20: Crosstalk and luminance variations along the projection axis, z, for diffuser 1 (a) and 2 (b) at the position (x,y) = (0,9)cm.

Figure 3.19a is the luminance map of viewer's space in projector plane. The luminance of the display decreases to 50% of the maximum luminance at around 420 mm away from the center of viewing slits, which are located at (0,0) in coordinate system. Thus, the FWHM length, L, of viewing slits is 840 mm. By placing the prototype parameters, stated in Table 3.2, into Eq. 3.2, the FWHM length, L, of viewing slits is calculated as 859 mm, which validates the experimental result of

840 mm.

Figure 3.20a shows the crosstalk, and luminance variations in projection axis. The crosstalk of the display is below 5 % for ± 7.5 cm away from the projector plane. Thus, the viewer still perceives stereo images away from the projector plane. However, as the viewer moves away from the projector plane, perceived luminance varies over the transfer screen.

In order to increase the viewing field by increasing the maximum rotation angle, θ, of viewing slits, another transfer screen has been constructed by replacing diffuser 1, $40^o \times 0.2^o$ aperiodic 1D diffuser, with diffuser 2, $20^o \times 0^o$ periodic diffuser. Crosstalk, and luminance maps of the viewer's space have been obtained for the screen with diffuser 2, and presented in Figs. 3.18b, 3.19b, and 3.20b. The crosstalk of the screen with diffuser 2 is less than the diffuser 1, for the same area of viewer's space, as presented in Fig. 3.18a. The maximum rotation angle, θ, of viewing slits is 58^o for the prototype 2, and it is more than the maximum rotation angle, θ, of viewing slits for the diffuser 1, which is 46^o. Figure 3.18d illustrates the horizontal cross-section of viewing slits for different rotation angles. As seen in Fig. 3.18d, the actual width, w, of viewing slits, which is the full width at 5 % of maximum intensity for 0^o of rotation, is around 60 mm. By placing the actual width, w, of viewing slit into Eq. 3.7, the maximum rotation angle, θ, of viewing slits is calculated as 61^o, which validates the experimental result of 58^o.

Figure 3.19b is the luminance map of viewer's space in projector plane for the the screen with diffuser 2. As seen in Fig. 3.19b, the luminance of the display decreases to 50% of the maximum luminance at around 210 mm away from the center of viewing slits. Thus, the FWHM length, L, of viewing slits is 420 mm. By placing the prototype 2 parameters, which are the projection distance, d, of 1180 mm, and the FWHM diffusing angle, ϕ, of 20^o into Eq. 3.2, the FWHM length, L, of viewing slits is calculated as 416 mm, which validates the experimental result of 420 mm.

As explained in previous paragraphs, theoretical analysis of the system characteristics and experimental results match each other. The length, L of viewing slits depends

on diffusing angle of 1D diffuser in transfer screen. Due to the system design structure, projected images passes through 1D diffuser twice. Thus, diffusing angle of diffuser must be multiplied with two and placed into Equ. 3.2. However, experimental results show that although there is double pass of light from diffuser, the effect of diffuser doesn't change significantly. In order to demonstrate the effect of double pass, a simple experiment has been conducted. A single beam of laser light has been sent onto single diffuser, light passed through diffuser once, and length of diffused light has been measured. For double pass, the same experiment has been repeated with two diffusers which are placed back to back, and with single diffuser with a mirror behind it. Two diffusers and single diffuser with mirror behind it gave the same length for diffused light which had double pass. However, length of diffused light for single diffuser is slightly smaller than the double pass experiment. The difference between single pass and double pass is smaller than the double. Thus, with little measurement error, the theoretical analysis and experimental analysis of system characteristics match each other. The effect of double pass on diffusing angle must be investigated as a further study.

Figure 3.20b shows the crosstalk, and luminance variations in projection axis for the screen with diffuser 2. The crosstalk for the diffuser 2 is less than the crosstalk for diffuser 1, for ± 7.5 *cm* away from the projector plane, as presented in Fig. 3.20a.

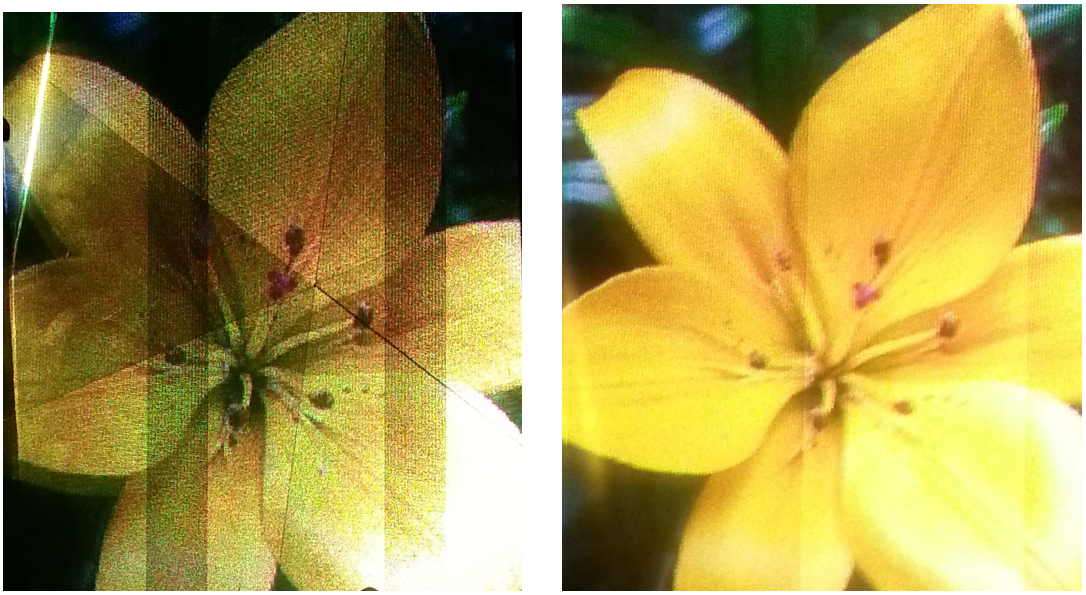

(a) (b)

Figure 3.21: Images captured from a screen with (a) periodic and (b) aperiodic diffuser, respectively. Moire artifacts are visible in the periodic screen.

As the periodic diffuser is used instead of aperiodic diffuser, the crosstalk of the display in viewer's space has decreased significantly. However, the mismatch between the periodicity of retro-reflector sheet, and the periodicity of 1D diffuser created Moiré patterns on transfer screen, as seen in Fig. 3.21a. Thus, the 1D diffuser must be aperiodic in order to have a Moiré-free transfer screen, as seen in Fig. 3.21b. Although the periodic diffuser creates Moiré patterns, subjects have stated that the display presents successful stereoscopic vision for both types of the 1D diffuser.

$$s = 2 \times d \times tan(\beta/2) \tag{3.9}$$

In projection-based displays, screen size, s, is determined by the projection distance, d, and the projection angle, β, as in Eq. 3.9. For the displays which project images on Lambertian scattering surfaces, the screen size, s, is limited by the projector's power, since as the projection distance, d, increases, the luminance of the display decreases dramatically.

As the screen in prototype is a high gain retro-reflective diffusing surface, all generated power is concentrated into the viewing slits, and luminance is always reasonably high in the viewing slits regardless of projection distance. Retro-reflective surfaces can have gains of between $1k - 10k$ [24]. Thus, projection distance, d, and screen size, s, is not limited by the projector power. However, it should also be noted that, as the retro-reflector screens work under a specific acceptance angle limit, projection angle, β can not exceed the acceptance angle limit. In the prototype, projection angle, β, is 28.4^o, which is smaller than the acceptance angle, 30^o, of retro-reflector.

3.4 Further Applications: Super Stereoscopy Technique for More Realistic 3D Display

The display proposed in the thesis study provides a pair of parallax images for two eyes which invoke 3D perception for the viewer without need of any glasses. Since the viewer perceives 3D images, viewer's eyes converges to the right position of objects in the presented image. However, viewer's eyes focus on the screen to see sharp images, as illustrated in Figs. 3.23(a) and 3.23(b). This is a conflict called as accomodation-vergence conflict. Almost all 3D displays suffer from this conflict which leads viewing discomfort for 3D displays especially when the virtual objects are closer than 0.5 m. For a possible new application and solving this conflict in the proposed display, a new technique that is named as Super Stereoscopy (SS3D) and developed by our group is tested with the proposed display, as reported in [3]. The detailed analysis of the technique is explained in [2].

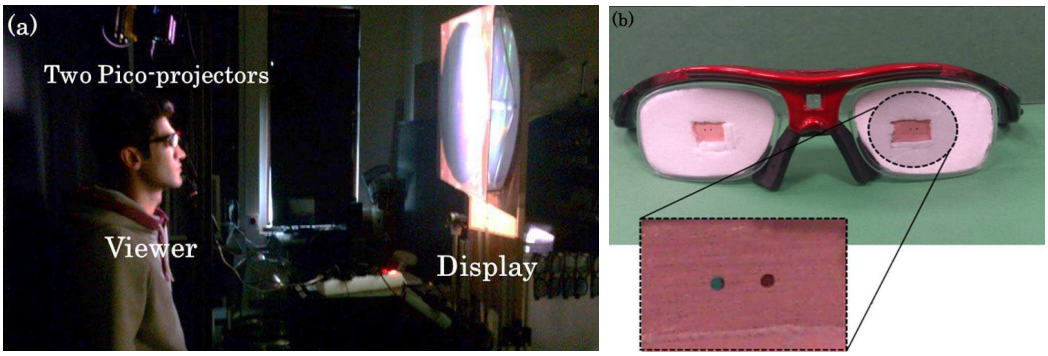

(a) (b)

Figure 3.22: (a) The proposed display used for testing and (b) created pinhole glass prototype with pinhole diameter of 0.6 mm and pinhole separation of 1.4 mm [2].

The proposed display is used as a test bench for this new SS3D technique, 3.22a. A prototype SS3D eyeglass is built to perform experimental tests in our lab 3.22b. On both sides of the eyeglass, there are two pinholes with embedded color filters. The pinholes have a diameter of 0.6 mm and a separation of 1.4 mm, with a red color filter on the left and a cyan color filter on the right (as seen from the viewers side). In order to solve accomodation-vergence conflict in the proposed display, the viewer of the proposed display wears this special SS3D glasses and a specially created stereo images are projected from the projectors. The SS3D technique and content creation are explained in the next paragraphs.

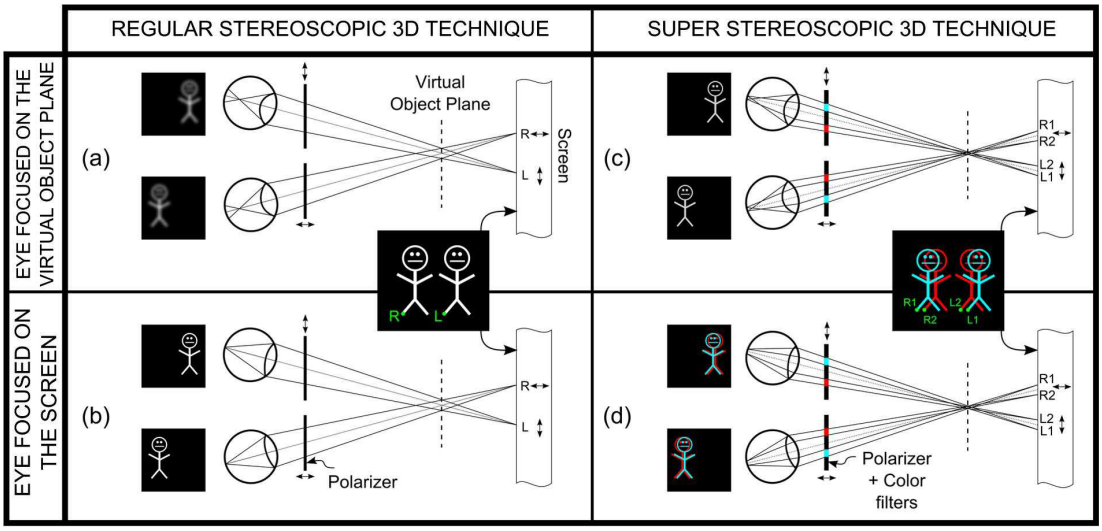

Figure 3.23: Retinal image formations in regular stereoscopic 3D and SS3D systems. (a) Blurred retinal images occured by accomodation of eyes on the virtual object plane. (b) Sharp retinal image by accomodation of eyes on the screen. (c) Sharp retinal images due to pinholes on SS3D glasses (Accomodation of eyes are on the virtual object plane). (d) Two seperated sharp parallax images results an approximate blur effect, [2].

As explained in [2], created stereoscopic glasses have pinholes which are smaller than the pupil of the eye. Through these pinholes, images are seen sharp wherever eyes are accommodated. Since accommodation doesn't affected by sharpness of images, eyes can accommodate where they converge. Thus, accommodation and convergence are in agreement and accommodation-vergence conflict is solved. In order to add natural blur for defocused objects, two pinholes for each eye are used. Two pinholes per eye have different light selective filters which allows to view two different parallax images per eye. Totally, there are 4 different parallax images. Two different parallax per eye overlaps and a single sharp retinal image is seen at the virtual object plane for a focused object, Fig. 3.23(c). For defocused object, two parallax images are seen sharp and slightly shifted from each other which gives an approximate blur effect, as seen in Fig. 3.23(d). Thus, while solving accommodation-vergence conflict, by given blur effect, 3D images appear more natural.

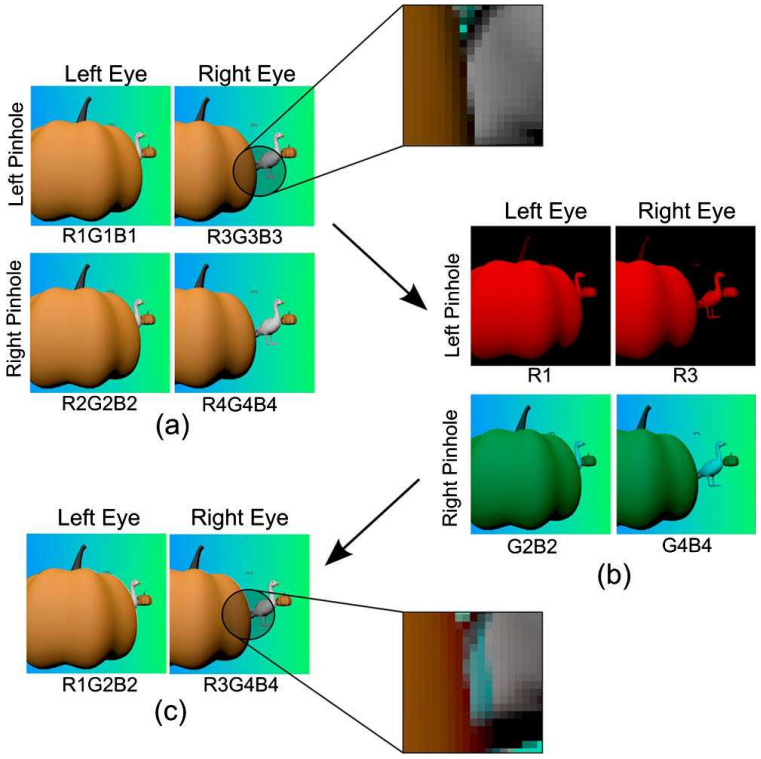

Figure 3.24: Content creation procedure. (a) 4 different parallax images (b) Images with corresponding colour channel (c) Superimposition of two parallax images, [2].

Fig. 3.24 illustrates how contents of SS3D are created. Every frame of the proposed display has 4 different parallax images, Fig. 3.24(a). Two of these images are projected by left projector, and the other two are projected by the right projector. Two parallax images projected by one projector have different colour channels from each other. Image passing through left pinhole of each eye has only red channel. Image passing through right pinhole of each eye has green and blue channels, Fig. 3.24(b). These two images with different channels are superimposed into a single image, then this image is projected by corresponding projector, Fig. 3.24(c).

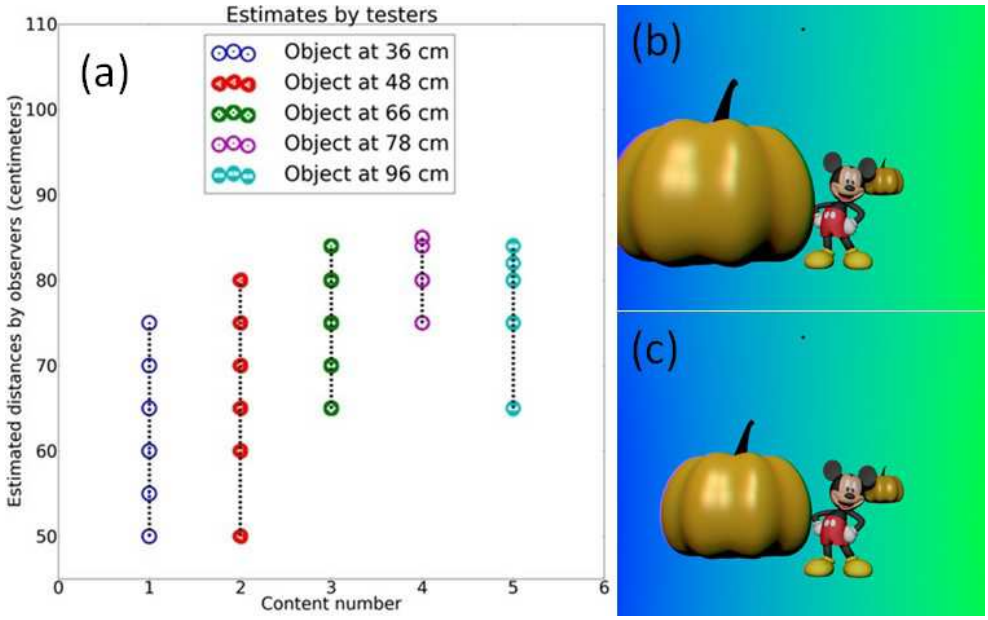

Figure 3.25: (a) Estimated distance by testers with different contents. (b) Right eye content of the object (pumpkin) at 36 cm (c) Right eye content of the object (pumpkin) at 48 cm. The image of the cartoon character appears on the screen at 1 m from the user [3].

Subjective test was conducted to investigate the proposed technique.A photograph of the test bench is showed in Figure 3.22a which the distance between the user and the screen is fixed at 100 *cm* through the tests. The subjects where chosen randomly among the university students and staffs. All the participants were young and were not using correction for their vision. In each case the users were first shown same standard images in order to see if the subject were experienced enough to distinguish a 3D image, to calibrate the white balance, and to apply the required alignment due to differences in their IPDs. All the images shown in the test were static 3D images. Viewers were asked to estimate the distance of 3D objects in the shown content. All images contained a reference point at infinite distance, which is used to register stereo pair correctly. Additionally, each image contained three different objects at different distances which two of them (the right pumpkin and the cartoon character) were fixed and one of them (the big pumpkin) was shown in different distances. Note that all of the images were created in-house using open-source 3D models in Blender rendering

software. Figure 3.25 shows the estimated distances by testers with different contents. Only 13% of subjects could perceive the most extreme content as 3D before using SS3D glasses, but with the help of our purposed 3D glasses this number increased to 100%. Major observed drawback of SS3D glasses during the test was found to be a decrease in brightness of the screen by testers. Another possible problem was resolution due to pinhole diffraction nature. As the distance between the viewer and the display increases, the pinhole or the alternative slit structure limits the smallest resolvable spot size to about 0.3 mm (at 500 mm subject distance).

As a conclusion, by introducing the new technique Super Stereoscopy and applying it to the proposed display, the accomodation-vergence conflict has been resolved in the proposed display and leaded to a new application area of the proposed display.

Chapter 4

CONCLUSION

A new type of multi-view autostereoscopic projection display, using a pair of laser based pico projectors with MEMS scanner, a pupil-tracking camera, and a rotating retro-reflective diffuser screen is proposed and demonstrated in the thesis. In order to realize proposed technique a prototype has been constructed. Different mechanical designs and different elements are tested with the prototype. Two different light diffusers, one is periodic diffuser and the other is aperiodic diffusers are tested in the transfer screen. Two different mechanical designs are applied in order to rotate the transfer screen. Theoretical analysis and experimental results of these different designs and elements are reported in the thesis and they are in good agreement.

A Python script is written in order to control the transfer screen in real time and to calibrate diffusing axis of the screen with initial position of mechanical unit. Another script is written to check the position of projectors with respect to pupil-tracker system since the prototype uses viewer's position with respect to projectors to rotate transfer screen.

The final prototype has a hexagonal shaped screen with 600 mm diagonal length. A viewing field of 700 mm in horizontal axis, and 500 mm in vertical axis with a crosstalk value below 5 %. The crosstalk remained below 5 % within ± 7.5 cm in the z-axis, i.e., user can move back and forth about 15 cm and the crosstalk remain at acceptable levels while the luminance dropped by 25 % and 10 %. Beyond that range, the luminance at the edges of the transfer screen decreases and corners of images are vignetted.

As a further application of the proposed display and a solution to the well-known problem of accomodation-vergence conflict in 3D displays, a new technique called as

Super Stereoscopy and developed by our group is applied to the proposed display. Subjective tests are performed and reported in the thesis. By applying Super Stereoscopy technique to the proposed display, the accomodation-vergence conflict has been resolved in the proposed display and leaded to a new application area of the proposed display.

The autostereoscopic projection display technique introduced in this thesis presents 3D images to a single viewer without need of any glasses. The technique is cost efficient since it uses only two projectors rather than an array of projectors to provide large viewing field. The screen size is scalable due to retro-reflector used in the screen. The technique provides high-gain, and sufficient brightness even with a pair of low lumen mobile projectors. There is no loss of 3D vision and discrete transition between different perspectives when the viewer changes his position. The transition between different perspectives is smooth as viewing slits track the eyes real-time. In the present method, since neither projectors nor screen make translational movement, projected images are always overlapped on the screen, and no distortion correction is required. Some but not all possible application scenarios for the proposed displays are personal entertainment displays used in transportation, training and entertainment simulators, interactive design tables, etc.

PUBLICATION RECORD

[O1] O. Eldes, K. Akşit, and H. Urey, "Multi-view autostereoscopic projection display using rotating screen," Optics Express **21**, 29043–29054 (2013).

[O2] O. Eldes, K. Akşit, and H. Urey, "Paper No 17.4: 3D Auto-stereoscopic display using pico-projectors and rotating screen," in "EURODISPLAY2013: 33rd International Display Research Conference, September," (SID, 2013).

[O3] O. Eldes, K. Akşit, and H. Urey, "Auto-Stereoscopic Projection Display using Head-Tracker and Rotating Screen," in "SID-ME 2014: Mid-Europe Chapter Sprint Meeting at Istanbul, April,"(SID, 2014).

[O4] O. ELDES, "Method for autostereoscopic projection Displays," (2015). WO Patent App. PCT/IB2013/056,842.

[O5] K. Aksit, A. Niaki, O. Eldes, and H. Urey, "Super stereoscopy 3d glasses for more realistic 3d vision," in "3DTV-Conference: The True Vision - Capture, Transmission and Display of 3D Video (3DTV-CON), 2014," (2014), pp. 1–3.

[O6] K. Akşit, , Osman. Eldes, S. Viswanathen, M. Freeman, and H. Urey, "Portable 3D Laser Projector using Mixed Polarization Technique," Journal of Display Technology **8**, 582–589 (2012).

[O7] K. Akşit, O. Eldes, S. Viswanathen, M. Freeman, and H. Urey, "Mixed Polarization 3D Technique for Scanned Laser Pico Projector Displays," in "IMID2012: The 12th International Meeting on Information Display, August," (SID, 2012).

[O8] K. Aksit, O. Eldes, M. K. Hedili, and H. Urey, "Paper no 15.1: Augmented reality and 3d displays using pico-projectors," SID Symposium Digest of Technical Papers **44**, 243–246 (2013).

[O9] H. Urey, S. Holmstrom, U. Baran, K. Aksit, M. Hedili, and O. Eldes, "Mems scanners and emerging 3d and interactive augmented reality display applications," (Invited talk in The 17th International Conference on Solid-State Sensors, Actuators and Microsystems, 2013).

[O10] H. Urey, K. Aksit, and O. Eldes, "Novel 3d displays using micro-optics and mems," in "International Conference on Fibre Optics and Photonics," (Optical Society of America, 2012).

[O11] K. Akşit, O. Eldes, and H. Urey, "Multiple Body Tracking for Interactive Mobile Projectors," in "IMID2012: The 12th International Meeting on Information Display, August," (SID, 2012).

BIBLIOGRAPHY

[1] K. Sakamoto and T. Morii, "Multiview 3d display using parallax barrier combined with polarizer," (2006), vol. 6399, pp. 63990R–63990R–8.

[2] K. Akşit, A. H. G. Niaki, E. Ulusoy, and H. Urey, "Super stereoscopy technique for comfortable and realistic 3d displays," Opt. Lett. **39**, 6903–6906 (2014).

[3] K. Aksit, A. Niaki, O. Eldes, and H. Urey, "Super stereoscopy 3d glasses for more realistic 3d vision," in "3DTV-Conference: The True Vision - Capture, Transmission and Display of 3D Video (3DTV-CON), 2014," (2014), pp. 1–3.

[4] N. Dodgson, "Autostereoscopic 3d displays," Computer **38**, 31–36 (2005).

[5] F. L. Kooi and A. Toet, "Visual comfort of binocular and 3d displays," Displays **25**, 99–108 (2004).

[6] O. ELDES, "Method for autostereoscopic projection displays," (2015). WO Patent App. PCT/IB2013/056,842.

[7] O. Eldes, K. Akşit, and H. Urey, "Multi-view autostereoscopic projection display using rotating screen," Opt. Express **21**, 29043–29054 (2013).

[8] R. Horstmeyer, "Spotlight Summary on Multi-view autostereoscopic projection display using rotating screen," `https://www.osapublishing.org/spotlight/summary.cfm?id=274600` (2013). Spotlight On Optics.

[9] H. Urey, S. Holmstrom, U. Baran, K. Aksit, M. Hedili, and O. Eldes, "Mems scanners and emerging 3d and interactive augmented reality display applications," (Invited talk in The 17th International Conference on Solid-State Sensors, Actuators and Microsystems, 2013).

[10] O. Eldes, K. Akşit, and H. Urey, "Paper No 17.4: 3D Auto-stereoscopic display using pico-projectors and rotating screen," in "EURODISPLAY2013: 33rd International Display Research Conference, September," (SID, 2013).

[11] O. Eldes, K. Akşit, and H. Urey, "Auto-Stereoscopic Projection Display using Head-Tracker and Rotating Screen," in "SID-ME 2014: Mid-Europe Chapter Sprint Meeting at Istanbul, April," (SID, 2014).

[12] S. Battersby, "Autostereoscopic display apparatus," (2000). US Patent 6,069,650.

[13] S. Hines, "Projected autostereoscopic lenticular 3-d system," (2011). US Patent 7,874,678.

[14] D. Ezra, G. Woodgate, J. Harrold, and B. Omar, "Three-dimensional projection display apparatus," (1997). US Patent 5,703,717.

[15] S. Shestak, "Multi-view autostereoscopic projection system using single projection lens unit," (2010). US Patent 7,699,472.

[16] C. Gao and J. Xiao, "Retro-reflective light diffusing display systems," (2011). US Patent 7,993,016.

[17] H. Baker and Z. Li, "Camera and projector arrays for immersive 3d video," in "Proceedings of the 2Nd International Conference on Immersive Telecommunications," (ICST (Institute for Computer Sciences, Social-Informatics and Telecommunications Engineering), ICST, Brussels, Belgium, Belgium, 2009), IMMERSCOM '09, pp. 23:1–23:6.

[18] P. V. Harman, "Autostereoscopic teleconferencing system," (2000), vol. 3957, pp. 293–302.

[19] K. Akşit, "Next generation 3d display applications using laser scanning pico projectors," Ph.D. thesis, Koc University (2014).

[20] I. Microvision, "Microvision: A World of Display and Imaging Oppurtunities," `http://www.microvision.com` (2012).

[21] K. Akşit, "kunguz/osman," `https://github.com/kunguz/osman` (2012).

[22] A. J. Woods, "How are crosstalk and ghosting defined in the stereoscopic literature?" (2011), vol. 7863, pp. 78630Z–78630Z–12.

[23] F. L. Kooi and A. Toet, "Visual comfort of binocular and 3d displays," Displays **25**, 99 – 108 (2004).

[24] P. V. Harman, "Retroreflective screens and their application to autostereoscopic displays," (1997), vol. 3012, pp. 145–153.